

Distribution and characteristics of supraglacial channels on mountain glaciers in Valais, Switzerland

Holly Wytiahlowsky¹, Chris R. Stokes¹, Rebecca A. Hodge¹, Caroline C. Clason¹, Stewart S.R. Jamieson¹

¹Department of Geography, Durham University, Durham, DH1 3LE, United Kingdom

Correspondence to: Holly Wytiahlowsky (holly.e.wytiahlowsky@durham.ac.uk)

Abstract. Supraglacial channels form a key component of glacier hydrology, transporting surface meltwater to englacial and proglacial positions, which impacts ice flow dynamics, surface mass balance and the hydrochemistry of glacial runoff. The presence of supraglacial channels is well-documented on ice sheets using satellite imagery, but much less is known about their properties on mountain glaciers. Here we use high-resolution (0.1 m) orthophotos to identify channels across 285 glaciers in Valais Canton, Switzerland. For the 85 glaciers with visible supraglacial drainage networks, we map 1890 channels (> 0.5 m wide) and investigate their distribution and characteristics. We find glacier hypsometry, size, that mean elevation and slope are good predictors of exert the strongest influence on glacier drainage density, with glaciers characterised by shallow slopes (which have fewer crevasses) and larger snow-free areas (with a high a large portion of their area at lower elevations (resulting in a higher meltwater supply) exhibiting higher drainage densities. The strongest control on drainage density There is mean glacier elevation, with glaciers at lower elevations producing higher drainage densities, also significant inter-glacier variability in channel termini locations. On average, 80 % of channels drain across the glacier surface and directly onto proglacial areas, with only 20 % terminating englacially. However, there is large inter-glacier variability, with 4048 % of glaciers containing contain no englacially-terminating channels and 3.5 % where all of glaciers host channels that all terminate englacially. Most Lastly, most channels on glaciers in Valais are only slightly sinuous, with higher sinuities typically occurring in flatter areas and associated with patchy debris cover. Future research should assess the importance of channels below our mapping resolution and network evolution under climate change investigate how drainage networks may evolve under continued climatic warming.

Formatted: Font: Bold

1 Introduction

Glaciers and ice caps are losing mass rapidly (Wouters et al., 2019; Hugonnet et al., 2021; Tepes et al., 2021; The GlaMBIE Team, 2025), resulting in sea level rise, which is anticipated to continue throughout the 21st century and beyond (Bamber et al., 2019; Edwards et al., 2021; Rounce et al., 2023). Glaciers in the lower latitudes (e.g., the European Alps, Caucasus, New Zealand, the USA) are particularly vulnerable to atmospheric warming and may experience complete deglaciation by 2100 under a strong warming scenario (e.g., RCP8.5) (Zekollari et al., 2019; Rounce et al., 2023). In populated mountain regions, these changes will have profound impacts, as glaciers and snowpacks act as vital water towers, supplying freshwater to the 1.9 billion people worldwide who live in or

downstream of glacial catchments (Carey et al., 2017; Zemp et al., 2019; Immerzeel et al., 2020; Sommer et al., 2020; Hugonnet et al., 2021; Clason et al., 2023). Glacier meltwater that feeds proglacial rivers is commonly transported to the proglacial margin by supraglacial channels, which are an important component of the glacial hydrological system. The presence and distribution of supraglacial channels have implications for a range of glacio-hydrological processes as they affect how efficiently meltwater is routed over, through and under glaciers, and can also affect suspended sediment concentrations and hydrochemistry of proglacial rivers. Higher suspended sediment concentrations pose harm to downstream ecosystems and proglacial reservoirs, with concentrations generally higher if meltwater is routed via the bed (Swift et al., 2002), rather than transported across the glacier surface. The presence or absence of channels that route meltwater to the bed also affects the supply of subglacial meltwater, which has implications for subglacial water pressure, the onset of subglacial channelisation and, potentially, ice motion (e.g., Willis, 1995; Jobard and Dzikowski, 2006; Banwell et al., 2016). Despite the importance of meltwater routing, the controls and patterns of meltwater transport on mountain glaciers remain relatively understudied compared to, for example, the Greenland Ice Sheet (GrIS). Notably, ~~the spatial distribution of supraglacial channels~~ is not yet fully understood ~~why the channelised flow of meltwater occurs on some glaciers but not others~~ (Pitcher and Smith, 2019), ~~nor are the controls on their distribution.~~

The term ‘supraglacial stream’ was first coined in the 1970s and 1980s from observations of channels in Scandinavia and the European Alps (e.g., Knighton, 1972, 1981, 1985; Ferguson, 1973; Hambrey, 1977; Seaberg, 1988), with their morphology (i.e., channel shape and structure) often compared to terrestrial streams. However, these early studies only provided small-scale, local observations of channels on individual glaciers. By comparison, a recent revival in supraglacial channel research has primarily focused on large-scale remote-sensing observations of the GrIS (e.g., Smith et al., 2015; Karlstrom and Yang, 2016; Gleason et al., 2021; Yang et al., 2015, 2016, 2018, 2019, 2020, 2021, 2022), and, to a lesser extent, Antarctica (e.g., Bell et al., 2017; Kingslake et al., 2017; Chen et al., 2024). Recent remote sensing techniques for channel detection on the GrIS (e.g., Yang and Smith, 2013; King et al., 2016) have rarely been applied to mountain environments, as most channels on mountain glaciers are likely ~~much smaller and therefore to be smaller than those on the GrIS. Observations are limited to very small sample sizes but have shown that they tend to be less than a metre wide (Knighton, 1972, 1981, 1985; Ferguson, 1973), and would, therefore,~~ fall below the resolution of even the highest-resolution freely available satellite platforms (e.g., Sentinel-2, ~10 m). As a result, it is not known whether the characteristics of channels on ice sheets and the controls on their distribution are comparable to ~~channels~~those on mountain glaciers. ~~The latter Mountain glaciers are characterised by less also limited in the surface area available space for channel formation, (compared to ice sheets),~~ tend to have a larger debris coverage, and typically contain steeper and more complex topography compared to ice sheet surfaces. ▲

Whilst much remains ~~unknown to be known~~ about supraglacial channel distribution in mountainous environments, ~~(i.e., where they form and their densities),~~ previous research has established some fundamental principles (e.g., Knighton, 1972, 1981; Ferguson, 1973; Yang et al., 2016). The formation of supraglacial channels is thought to occur when channel incision via thermal erosion exceeds the rate of surface lowering (Marston, 1983). Channel formation is also influenced by ~~the rate of meltwater production and~~ surface topography, with channels tending to form parallel to the steepest ice flow direction (Irvine-Fynn et al., 2011; Mantelli et al., 2015). ~~On a smaller scale, micro- to macro-scale structures have also been suggested to influence meltwater routing (Irvine-Fynn et al.,~~

Formatted: Font color: Auto

2011), and areas of higher roughness appear to be correlated with, and may be caused by, higher channel densities (Rippin et al., 2015). Surface topography may reinforce itself, as once an incised channel forms, the higher incision rates may result in an increasingly topographically constrained channel that reactivates annually. At a smaller scale, micro-to-macro-scale surface structures have been suggested to influence meltwater routing (Irvine-Fynn et al., 2011), while high supraglacial channel density appears to be correlated with, and may contribute to, increased surface roughness. Incision rates typically increase with discharge and (Rippin et al., 2015). Where channels occur, they are often reactivated annually depending on their depth, with the most deeply incised channels suggested to be a product of high discharge or high slope (St Germain and Moorman, 2019). However, incised channel profiles are not typically uniform, and most channels commonly exhibit asymmetric cross-profiles due to the dominant direction of solar radiation (St Germain and Moorman, 2019). Additionally, discharge is thought to be a strong control on channel form, especially sinuosity, with channels observed to increase in sinuosity throughout the melt season (e.g., Dozier, 1976; Hambrey, 1977; St Germain and Moorman, 2019). Similar to terrestrial river networks, supraglacial channels generally follow Horton's laws, meaning that higher-order channels (i.e., where the highest-order is the main channel) are longer, have lower slopes, and are comprised of a lower number of channel segments (Horton, 1945; Yang et al., 2016). However, much of what we know about supraglacial channels was established from cold-to-polythermal glaciers or from observations of a small number of individual glaciers, especially those that are cold-based or polythermal (e.g., Knighton, 1972, 1981, 1985; Gleason et al., 2016; St Germain and Moorman, 2019).

In this paper, we investigate a range of potential controls on channel distribution and properties for a large sample of glaciers ($n = 285$) in a region characterised by high melt rates. We use high-resolution (~ 0.1 m) orthophoto imagery from 2020 to produce the first comprehensive inventory of 1,890 supraglacial channels in a mountain glacier environment, with a focus on Valais Canton, Switzerland. Our aim is to characterise the morphometry (i.e., quantitative measurements of channel geometry) of supraglacial channels on mountain glaciers, providing insight into where and why they form. This is important for understanding how mass is transported through and away from glaciers, and for determining the extent to which surface hydrological characteristics (e.g., channel transport pathways) are uniform between glaciers, which is beneficial for informing modelling of glacier hydrology and ice motion. Using GIS software, we extract channel metrics (length, sinuosity, slope, elevation, terminus type, proximity to debris) and glacier surface characteristics (aspect, size, drainage density, elevation, crevassed extent), which are supplemented by qualitative observations of channel morphology and distribution. We then explore the relationship between glacier and channel characteristics using statistical measures and infer whether glacier surface characteristics can explain the presence or absence of channels.

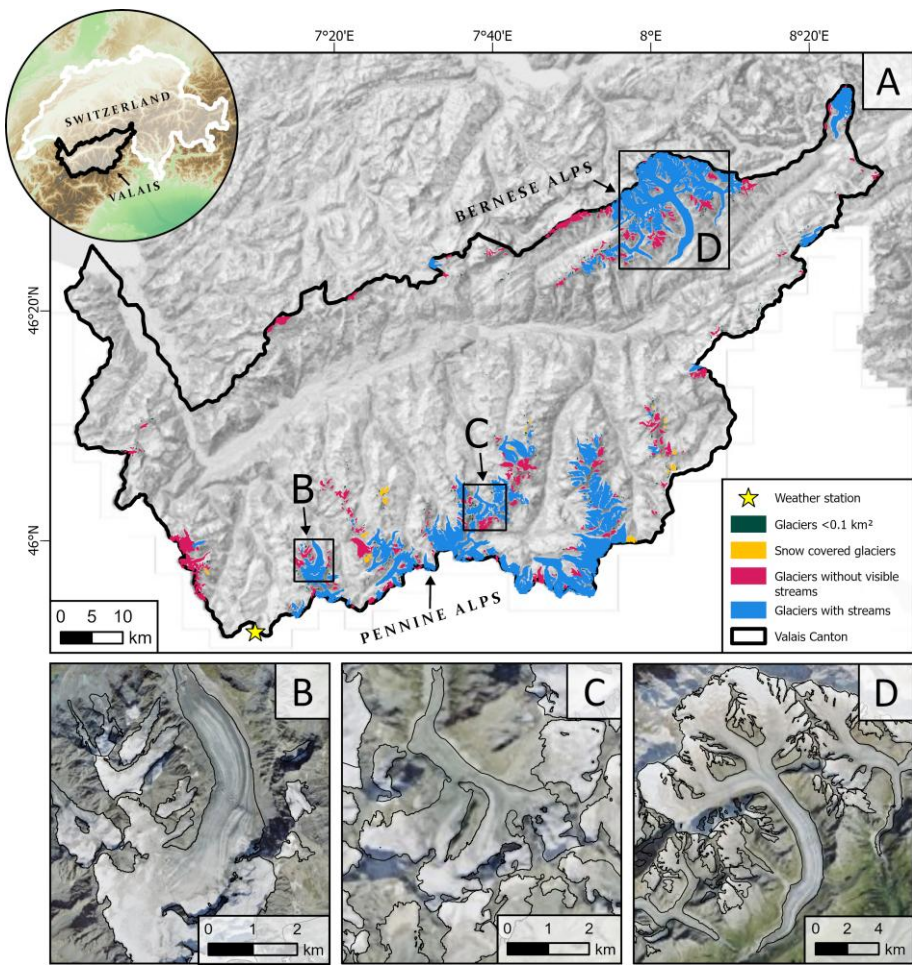
2 Study location

Compared to many glacierised regions, Switzerland has the largest repository of high spatial and temporal resolution national LiDAR and orthophoto surveys, providing excellent coverage for the mapping of supraglacial channels. We focus on Valais Canton in southern Switzerland, which contains 303 glaciers over 0.1 km^2 , covering a total area of 545 km^2 in 2015 (Fig. 1; Linsbauer et al., 2021). It is the most glacierised Swiss Canton, and in 2015, glaciers in Valais had a mean area of 1.8 km^2 , a median of 0.43 km^2 and a maximum area of 77.3 km^2 .

Formatted: Font color: Auto, English (United Kingdom)

Formatted: Font color: Auto

112 (Grosser Aletschgletscher) (Linsbauer et al., 2021). We identified the Valais Canton as a suitable study site
 113 as because its glacier size distribution is comparable with Switzerland to that of Switzerland as a whole, and the
 114 glaciers range from shallow to steep gradients, have differing hypsometries (ice area-elevation distributions), and
 115 varying crevasse densities. Thus, this study site captures a wide range of potential influences on channel
 116 distributions and characteristics. Valais is comprised of the Bernese Alps to the north and the Pennine Alps in the
 117 south, separated by the Rhône Valley (Fig. 1). Glaciers in the Bernese Alps are the largest in the canton and most
 118 exhibit a south-to-southeast aspect (mean: 163°). In contrast, the largest glaciers in the Pennine Alps have a north
 119 and west aspect (mean: 347°). Glaciers in Valais have an average maximum elevation of 3450 m a.s.l. (min: 2356,
 120 max: 4599) and an overall mean elevation of 3091 m a.s.l. (min: 2267, max: 4025).



121
 122 **Figure 1: The study site area, which contains 303 glaciers > 0.1 km². (A) The location of Valais Canton**
 123 **(black) is shown within southwest Switzerland. Glaciers containing visible streams (> 0.5 m wide) are shown**

in blue, glaciers without visible streams are in pink, glaciers fully covered by snow are in yellow, and all glaciers $< 0.1 \text{ km}^2$ (which we omit from this study) are shown in dark green; (B) an example of a large valley glacier (Glacier de Corbassière), with smaller glaciers at higher elevations; (C) the debris-covered tongue of Glacier du Grand Cornier and surrounding smaller glaciers; and (D) the larger glaciers (e.g., Grosser Aletschgletscher, centre-right) in the north of Valais. The location of Col du Grand St-Bernard meteorological weather station is indicated by a yellow star. Glacier outlines used are from the Swiss Glacier Inventory (SGI2016), with glacier extent shown for 2015-16. The outlines are overlaid on basemap imagery sourced from Esri (2024).

Within Valais, the only meteorological station with a similar elevation to many glacier termini is Col du Grand St-Bernard (2472 m a.s.l.) in the Pennine Alps (Fig. 1), which (between 1991 and 2020) recorded mean July-August air temperatures (2 m) of 8.46°C , mean January temperatures of -6.9°C , and mean annual temperatures of -0.1°C . At Col du Grand St-Bernard, July-August averages 140136 mm of precipitation (1991-2020), with 12.7 days a month experiencing $> 1 \text{ mm}$ of precipitation, compared to a January average of 242 mm across an average of 12.9 days. However, Switzerland's climate is changing and mean air temperatures between 2013 and 2022 were 2.5°C warmer than pre-industrial temperatures (MeteoSwiss, 2024), which has greatly impacted the mass balance of Swiss glaciers in recent decades (Fischer et al., 2015; Davaze et al., 2020).

3 Methods

3.1 Imagery acquisition and channel delineation

The method commonly used for automated channel detection, developed by Yang and Smith (2013) for delineating water bodies on the GrIS from WorldView-2 imagery (1.84 m), uses a normalised difference water index adapted for ice (NDWI_{ice}). Following Yang and Smith (2013), we applied a modified NDWI_{ice} approach to a high-resolution (0.1 m) orthophoto tile (1 km by 1 km) on the Grosser Aletschgletscher. However, our NDWI_{ice} output predominantly detected water-filled crevasses, and whilst it was able to detect some channels $> 0.5 \text{ m}$ in width, it typically identified only the largest channels (mostly $> 1 \text{ m}$). It also missed many channels that were visible but contained very small amounts of water, or incised channels where the water surface was not visible. This method is likely better suited to coarser imagery (less visible crevasses) in less complex terrain and/or for simply using a threshold to extract higher-order channels. As a result, we undertook manual mapping, which in some instances is sevenfold more accurate in ascertaining channel density compared to automated methods (King et al., 2016).

We obtained high-resolution cloud-free orthophoto imagery (0.10 m resolution) from SwissTopo (swisstopo.admin.ch), with which is primarily comprised of imagery acquired in August 2020 (5th, 7-8th, 15th, 21st and 27th). The remaining area is covered by imagery captured on the 4th of September, including a few small glaciers in southwest Valais and part of the Grosser Aletschgletscher's ablation area, which, despite their later acquisition dates during mid-July 2020. Imagery, do not appear to have abnormally high drainage densities. All imagery was not available for later-incaptured toward the end of the 2020 melt season, which lasted from approximately April to September 2020 at Col du Grand St-Bernard. Hence, our data is unlikely to capture the

peak extent of channel distribution, which is expected to occur in late summer, when mean monthly temperatures were above 0 °C at Col du Grand St-Bernard. Snow conditions at Col du Grand St-Bernard in mid-July during summer 2020 were likely to be lower than average, as the precipitation of the preceding winter (total across December, January, February) was 570 mm compared to the 2010 to 2020 mean of 704 mm. May temperatures were slightly warmer than average (2020 mean: 3.4°C; 2010-20 mean: 1.7°C), followed by a colder than average June (2020 mean: 4.8 °C; 2010-2020 mean: 6.3 °C), meaning that whilst there was less snow in winter, it may have melted more slowly than previous years.

We first removed all glaciers in Valais smaller than 0.1 km² from our study sample (582 reduced to 303 glaciers). This is because they are likely too small to produce form channels large enough channels to be detected by our imagery, and because many of the small glaciers listed in the Swiss Glacier Inventory (SGI2016) are unlikely to meet the criteria to be identifiable for classification as glaciers (Leigh et al., 2019). Due to the date of imagery acquisition, 6 % of the remaining 303 glaciers were still completely snow-covered and were omitted from further analyses as the presence or absence of channels could not be detected, leaving 285 glaciers. Within these glaciers, the mean snow-free area was 38.9 % in mid-July/August/September 2020, with some variation in snow cover across different elevation bands. For example, glaciers with a mean elevation between 2500 and 2800 m a.s.l. had a 45.0 % average snow-free area on average of 45.0 %, compared to 36.6 % at elevations between 3100 and 3400 m a.s.l. The lowest percentage of snow-free area was 4.9 % at a high elevation cirque, and five glaciers were completely snow-free by mid-July/August/September, but were all under 0.7 km².

Each glacier was systematically surveyed for supraglacial channels in QGIS (e.g., Fig. 2). Of the 285 glaciers that we surveyed, 85 supported supraglacial channels above our mapping threshold. Only channels confidently visible at a 1:1,000 scale were delineated for the purpose of consistency, meaning the minimum channel width we delineated was ~0.5 m. We solely focus on these larger channels because of difficulties in delineating small channels objectively, which include problems with differentiating complex rill networks from structural features (e.g., fractures). Additionally, smaller channels may have widths that periodically fall below the pixel resolution, which may require subjective judgments to be made. Whilst we do not map channels below the scale defined above, many of the glaciers likely contain smaller channels that are not sufficiently clear enough to map. These smaller channels may form a key hydrological component of these glaciers, but we anticipate that the channels we have mapped carry the bulk of the meltwater. Individual channels were mapped from their downstream end until they were no longer clearly visible or when channels could not be confidently and objectively mapped. When channels have tributaries above the mapping resolution, the main channels were mapped as one segment, continuing up the largest channel at each confluence. Each tributary channel was then subsequently mapped as a new individual segment. Once mapped, each entire channel segment was assigned a code based on its attributes and whether it was on bare ice, surrounded by patchy debris, or on a debris-covered part of the glacier. The type of terminus was assigned to each channel, which was one of: running off the glacier terminus, terminating in a moulin, crevasse, lake, the glacier periphery, adjoins another channel, or disappears beyond the resolution (i.e., the channel terminus is not visible and cannot be confidently inferred).

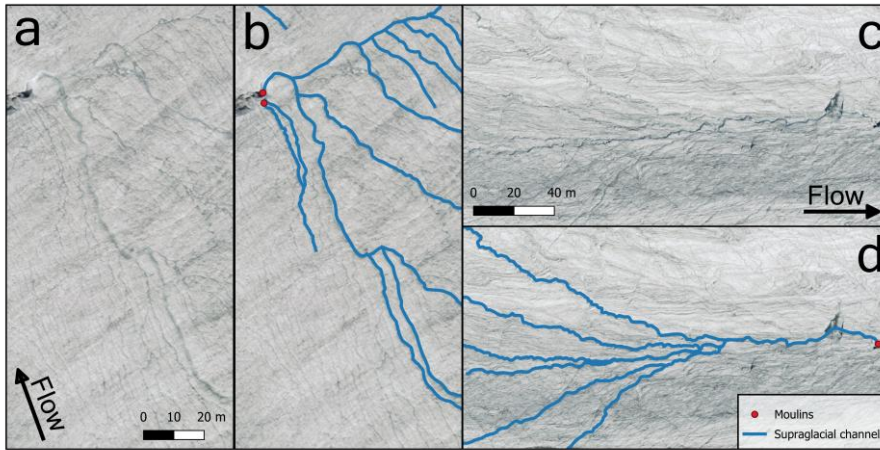


Figure 2: Examples of the mapped output and corresponding orthophoto. Channels are shown in blue, and moulins are represented by red circles when a mapped channel is moulin-terminating. Arrows indicate the direction of ice flow. (a-b) Supraglacial channels on the Glacier de Moiry (a-b) and (c-d) for Allalingletscher. (c-d). Imagery source: Federal Office of Topography Swisstopo.

To ensure consistency, all mapping and the error assessment were conducted by the same individual. We quantified the repeatability of our mapping by re-delineating channels from the same image of the Rhonegletscher on two occasions used in our original mapping, months apart after mapping was completed. This revealed a 2.6 % difference in calculated drainage density and a 0.21 % decrease in total channel length from compared to the original mapping (Figure Fig. B1). The error from our repeat mapping may have been lower if the mapping had been repeated immediately after the original mapping, whereas the original mapping was conducted consistently over a time span approximately 6-month period. However, the error margin is small enough for us to conclude that the original mapping provided a good representation of each glacier's drainage density. Both sets of mapping also clearly identified where channels terminate. The primary source of uncertainty here stems from knowing when to stop mapping up-channel and the total channel length. We therefore took a conservative approach to avoid over-interpreting channel pathways and only mapped the up-glacier channel limit of channel to where we were confident that it exists.

3.2 Metrics

A total of 1890 channel segments (polylines) were mapped across the 85 glaciers that contained channels. We then used the high-resolution (0.5 m) SwissALTI3D DEM (2019) from swisstopo.admin.ch (1 sigma accuracy of ± 0.3 m for each dimension) to extract morphometric characteristics from each channel segment. The DEM is coarser than the orthophotos used for channel delineation, and there is a one-year offset between their acquisition dates. However, as the DEM is used to calculate larger-scale metrics such as elevation and slope, the small offset we consider the difference in acquisition dates to be short enough that it is unlikely to affect the overall results, which

focus on relative differences in elevation, both on and between glaciers, rather than absolute values. Additionally, the DEM closely reflects the glacier surface topography at the time of mapping, and no major changes are observed over that year. Extracted channel metrics were included geodetic segment length, obtained from ArcGIS without a DEM input, and straight-line distance, elevation (calculated from DEM-derived minimum and maximum), elevation difference, and elevations. Elevation differences and segment length were used to calculate channel slope. The start and end points of each segment were then used to derive the We also calculated sinuosity for each segment (channel length¹ divided by straight-line distance) and, together with the total channel length per glacier, which was used to calculate glacier drainage density for each glacier (total channel length of channels divided by glacier area). We For glacier drainage density, we used the glacier-snow-free glacier area at the time of mapping to calculate drainage density, which resulted in a yielded higher value values than if the entire glacier area had been used.

Glacier characteristics were obtained from the Swiss Glacier Inventory (SGI2016), which included glacier area, aspect, and elevation (minimum, maximum and mean) in 2015 (Linsbauer et al., 2021). This record is the most up-to-date record inventory of Swiss glacier area, but glaciers have since undergone substantial recession. Glacier slope values from the SGI2016 cannot be used as they encompass the whole glacier, whereas for our analysis, which provides full coverage of all Valais glaciers in 2015 (Paul et al., 2019). From this inventory, we wanted to measure the slope of the snow-free portion of the ablation area at the time of channel mapping. To calculate slope values, extracted aspect and elevation data to characterise each glacier polygon was clipped to in its entirety, and only these values are used when referencing glacier elevation and aspect throughout. However, glacier area and slope refer only to the snow-free portion as this represents the area available for channel formation at the time of image acquisition. To calculate snow-free area, and then values, we clipped the 2015 glacier polygons at their snowline and extracted the snow-free area and slope (mean, minimum, and maximum) using zonal statistics in QGIS were used to extract the mean, minimum and maximum slope value from the Swiss ALTI3D DEM for each polygon. The snow-free slope value is the only glacial slope value used in data analyses. We. Additionally, we assigned codes to each glacier based on the size of the crevassed area due to its potential impact on channel formation. This included the following classes: little to no crevasses (less than 10 % of the snow-free area), moderately crevassed (10-50 % covered), and heavily crevassed (covers > 50 % of the snow-free area).

Formatted: Font: Not Italic

3.3 Statistical tests

To determine whether there is a relationship between channel morphometry and glacier characteristics, we produced a correlation matrix using Spearman's rank correlation (ρ) (e.g., St Germain and Moorman, 2019). Each metric used in this analysis comprises 1890 values, each representing an individual channel segment. The analysis used the following channel variables: segment length, channel slope, sinuosity, minimum elevation, maximum elevation and elevation range, and as well as the following glacier variables: drainage density, glacier area, mean slope of the snow-free area, aspect, glacier minimum elevation, glacier mean elevation, and glacier maximum elevation, snow-free area, and its mean slope. For each of the glacier variables, all channel segments on the same glacier were allocated the same value. A singular one-way ANOVA test was conducted performed to determine the significance of the relationship between the three debris-cover classes and sinuosity, as an ANOVA test is best

suited to determining if there is a significant difference between different classes of debris cover. We also conducted. In addition, a Principal Component Analysis (PCA) was conducted to determine the relationships between the variables used in our correlation matrix and to identify the main drivers of variance amongst the dataset, with data normalised to aid in identifying patterns within the data. enhance pattern detection. A secondary PCA and cluster analysis were also conducted to further explore relationships between glacier properties. Unsupervised k-means clustering was used to separate glaciers based on their slope, elevation (minimum, mean, maximum), drainage density, and channel termini locations. The resulting clusters were then visualised using a PCA biplot.

4 Results

4.1 Glacier observations

Glaciers with channels ($n = 85$) have a larger mean area than glaciers without channels ($n = 200$) (mean area = 5 km^2 vs. 0.6 km^2) and all glaciers larger than 5.6 km^2 contain channels $> 0.5 \text{ m}$ wide (Table 1, Fig. 3a). However, the modal glacier area is 0.1 to 1 km^2 for glaciers both with and without visible channels (Fig. 3a). Glaciers containing channels typically have lower slopes compared to those without channels (mean slope: 21° vs. 28°) (Fig. 3b). Glaciers with channels generally have longer tongues that terminate at lower elevations (mean minimum elevation = 2797 m vs. 2936 m) and have higher maximum elevations (mean max elevation = 3637 m vs. 3555 m). The mean drainage density of glaciers with channels is 2.4 km/km^2 and, with a maximum of 15.2 km/km^2 . The latter was found on Oberer Theodulgletscher, which has the lowest glacier slope in the dataset (13°) (Fig. 3c, Fig. 4a).

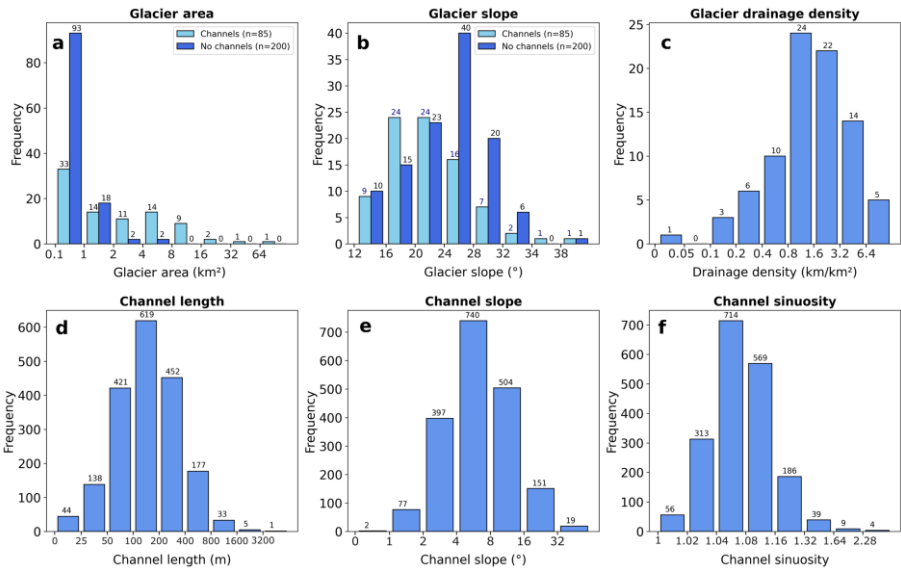
Table 1: Glacier and channel characteristics.

292 **Table 1: Glacier and channel characteristics.**

	Channel Length (m)	Channel Slope (°)	Sinuosity	Drainage Density (km/km ²)	Mean Glacier Slope (°)	Glacier Area (km ²)
Count	1890	1890	1890	85	85	85
Minimum	5.2	0.8	1.0	0	10.4	0.1
Median	152.2	6.3	1.1	1.5	20.6	1.5
Mean	211.7	8.0	1.1	2.4	21.0	5.0
Maximum	4314.4	47.8	3.8	15.3	43.0	83.0
Range	4309.3	47.0	2.8	15.2	32.6	82.9
Standard Deviation	228.3	6.3	0.1	2.6	6.5	10.7
Standard Error	5.3	0.1	0.0	0.3	0.7	1.2
Kurtosis	65.8	7.4	153.0	9.0	1.1	35.3
Skewness	5.5	2.3	9.5	2.6	0.8	5.4

Formatted Table

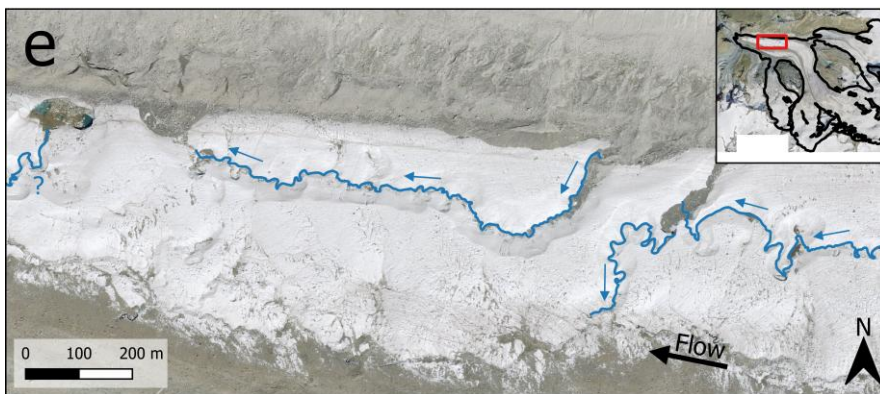
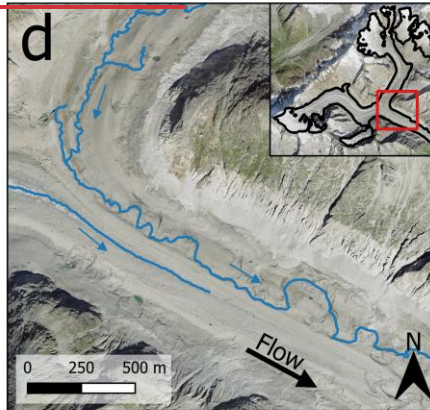
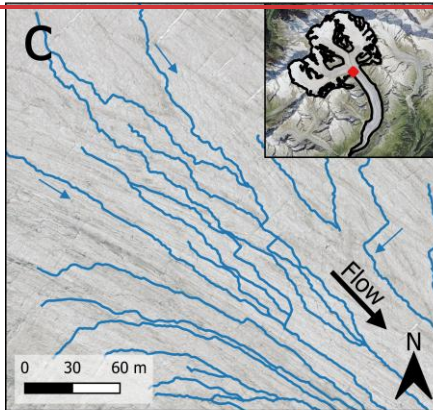
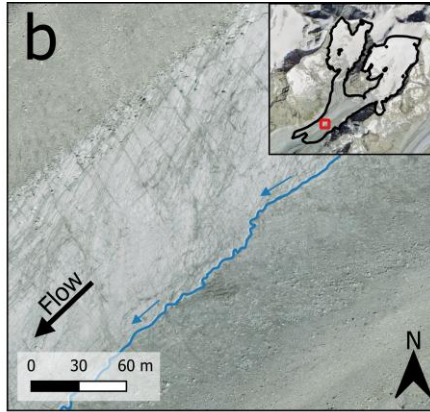
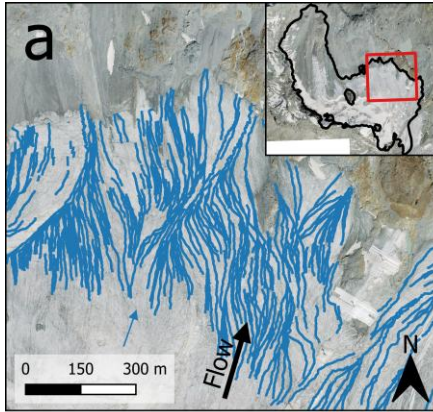
293



Formatted: Font: Bold

294

295 **Figure 3: Histograms of extracted metrics. Note that the x-axis uses a log scale (except for Fig. 3b) and the**
296 **numbers above each bar represent the number of channels/glaciers within each class. The range shown by**
297 **each bar is indicated by the x-axis values to either side. The range is exclusive of the lower value and**
298 **inclusive of the higher one (e.g., $> 1 - \leq 2$). (a) Glacier area (km²); (b) glacier slope (°); (c) glacier drainage**
299 **density (km/km²); (d) channel segment length (m); (e) channel slope (°); and (f) channel sinuosity.**



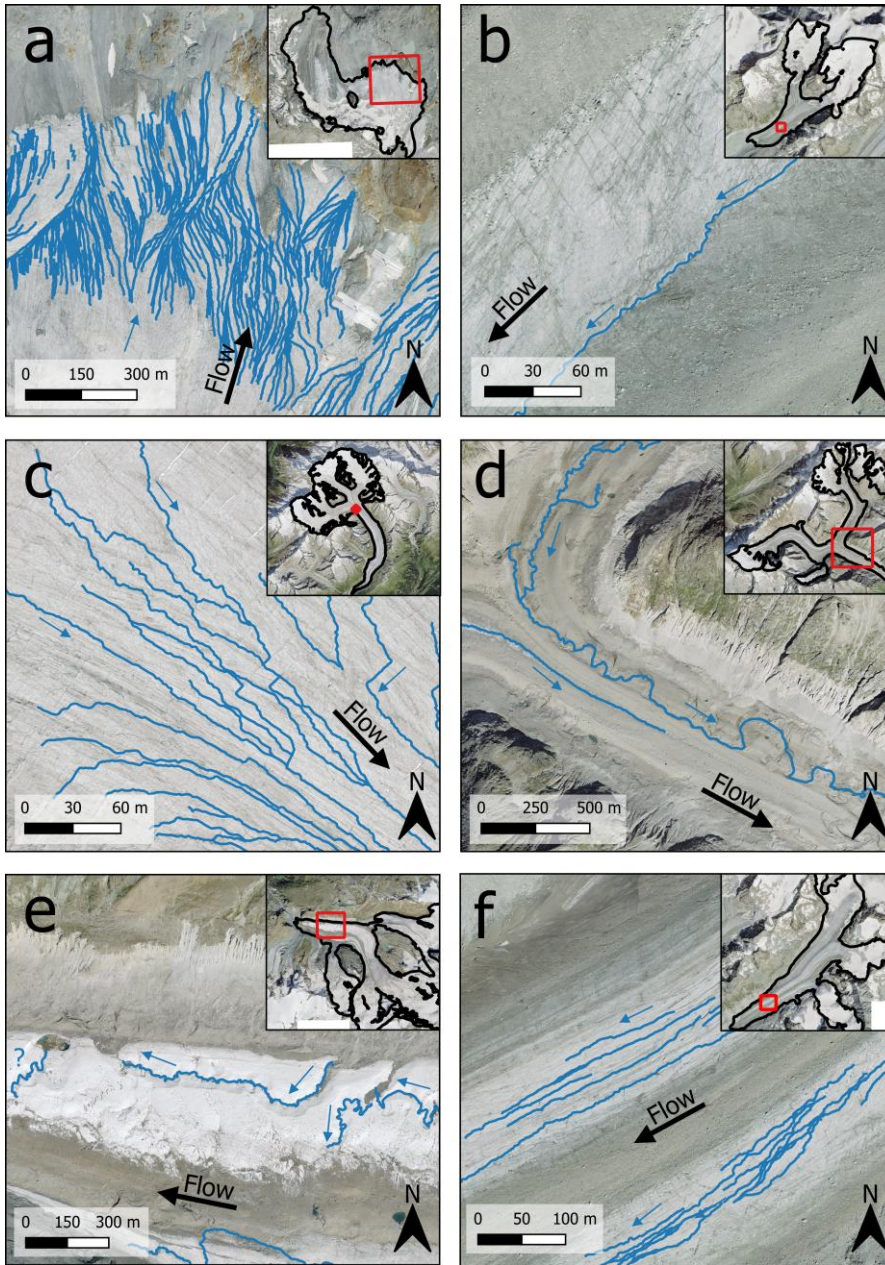


Figure 4: Examples of supraglacial channels. Channel location is shown in relation to the whole glacier in the top right of each panel, with the panel extent shown in red. (a) Channels on the Oberer Theodulgletscher; (b) a channel at the interface between bare ice and debris-covered ice on Glacier du

Brenay; (c) channels on the Grosser Aletschgletscher - note the straight segments where crevasses have been exploited; (d) channels on the debris-covered terminus of the Oberaletschgletscher; ~~and~~ (e) sinuous channels towards the terminus of Gornergletscher, including an example of a small supraglacial lake (left); ~~and~~ (f) channel networks on Glacier d'Otemma. The black arrows indicate the glacier flow direction, and the blue arrows indicate the water flow direction. A question mark is shown when the water flow direction is unclear in the DEM. Imagery source: Federal Office of Topography, Swisstopo.

4.2 Channel characteristics

Individual channel segments have a mean length of 212 m, with a positively skewed leptokurtic distribution (Fig. 3d; Table 1). Few segments exceed 1,600 m, as the snow-free areas of most glaciers are smaller than this. The channel segments have a mean slope of 8°, and most exhibit ~~a-slopeslopes~~ between 4 ° and 16° (Fig. 3e; Table 1). The maximum channel slope is 48°, but the overall distribution is positively skewed towards smaller slope values. The sinuosity index of each channel ranges from 1 (straight line) to a maximum of 3.8, with a mean value of 1.1, which is classified as sinuous (1.05 - 1.25), but not high enough to be defined as meandering (> 1.25) (Table 1) (Brice and Blodgett, 1978). Sinuosity is the most positively skewed variable, with a highly leptokurtic distribution, as most channels are not very sinuous (Fig. 3f).

Channels terminate in a range of settings, with 47 % joining another channel, 15 % terminating in crevasses, 14 % terminating in moulins, 13 % disappearing below the mapping resolution, 8 % running off at the glacier terminus, 2 % running off the side of the glacier, and 1 % terminating in a supraglacial lake (e.g., Fig. 4e). When only considering terminal segments (i.e., channels not adjoining another channel or disappearing below the mapping resolution), 72 % of segments terminate englacially (crevasses or moulins), 25 % run-off (glacier terminus or periphery), and 3 % terminate in a supraglacial lake. However, larger glaciers with higher drainage densities disproportionately impact these values. For example, 582 out of the 1890 mapped channel segments are on the Grosser Aletschgletscher, where no visible channels reach the terminus; hence, englacially terminating channels may be overrepresented by a single glacier. By comparison, ~~when the averageproportion of channels terminating in each location (i.e., englacially or running directly off the glacier within our terminus) at every glacier is averaged across the entire dataset, the resulting 'average' glacier~~ is characterised by 80 % of channels terminating proglacially and 20 % terminating englacially. Overall, 48 % of glaciers have no englacially-terminating channels; ~~(i.e., all channels remain supraglacial and run directly off the glacier)~~, with only 3.5 % of glaciers solely containing englacially terminating channels.

Qualitative observations suggest that ~~glacier surface properties and ice marginal features influence channel distribution and morphology~~ ~~are controlled by glacier structure and topography, and that channel networks display variation in drainage patterns across the dataset~~. For example, channels often occur along the interface between debris-covered and bare ice (e.g., Fig. 4b), particularly adjacent to ~~medial~~-moraines, where channels are confined to a topographic depression ~~or 'gutter', commonly occurring at the confluence between two tributaries; or at the ice margin~~. The influence of glacier ~~structuresurface features~~ on channel morphology is also observed where trace or shallow crevasses are exploited to produce long, straight channel sections (e.g., Fig. 4c). By comparison, the most sinuous channels tend to occur at low elevations ~~on large glaciers characterised by larger flat areas towards~~

Formatted: Font color: Auto

to their terminus (Fig. 4e), appear to be highly incised, and typically form on large flat areas close to the glacier terminus (Fig. 4e). Channel network patterns also vary, with some networks appearing more dendritic and interconnected (e.g., Fig. 4a), while others are more parallel and show reduced connectivity (e.g., Fig. 4f).

Formatted: Font color: Auto

4.3 Relationships between channel and glacier characteristics

Here, we investigate links between different supraglacial channel and glacier characteristics. Previous studies informed our choice of variables ~~tested to test~~ for potential relationships, with a focus on how glacier properties (slope, area and elevation) ~~affect~~ are related to glacier drainage density (e.g., Yang et al., 2016) and channel morphometry, such as sinuosity and channel segment length (e.g., St Germain and Moorman, 2019). We find that the most sinuous channels are more likely to occur on shallow slopes (0 to 10°), with channels on steeper slopes (> 20°) unlikely to exhibit a sinuosity over 1.3 (Fig. 5a). Statistically significant differences in channel sinuosity are also observed between our debris classes ($p < 0.05$; one-way ANOVA) (Fig. 5c). Channels on patchy ('proximal') debris cover tend to be the most sinuous and are statistically different ($p < 0.05$; Tukey Honest Significant Difference test) from channels on continuous debris cover ('debris') and those on bare ice ('clean'). The 'debris' class ~~is~~ generally contains more sinuous channels than the 'clean' class, but this difference is not statistically significant. Additionally, channel segment length tends to increase on shallower slopes (Fig. 5b). This relationship is clearly defined by an upper limit, where channels > 500 m are confined to slopes of < 20° and no channels occur on slopes > 50°, except for one outlier (Fig. 5b). Channel segments that terminate in moulins tend to be the longest (mean: 341 m, max: 1999 m), followed by channels that disappear below the mapping resolution (mean: 259 m, max: 4314 m), and then channels reaching the glacier terminus (mean: 214 m, max: 1193 m) (Fig. 5d). The very few (1 %) channels that terminate in supraglacial lakes tend to be short (mean: 109 m, max: 260 m), as do channels that adjoin a higher-order channel (mean: 169 m, max: 1174 m) (Fig. 5d).

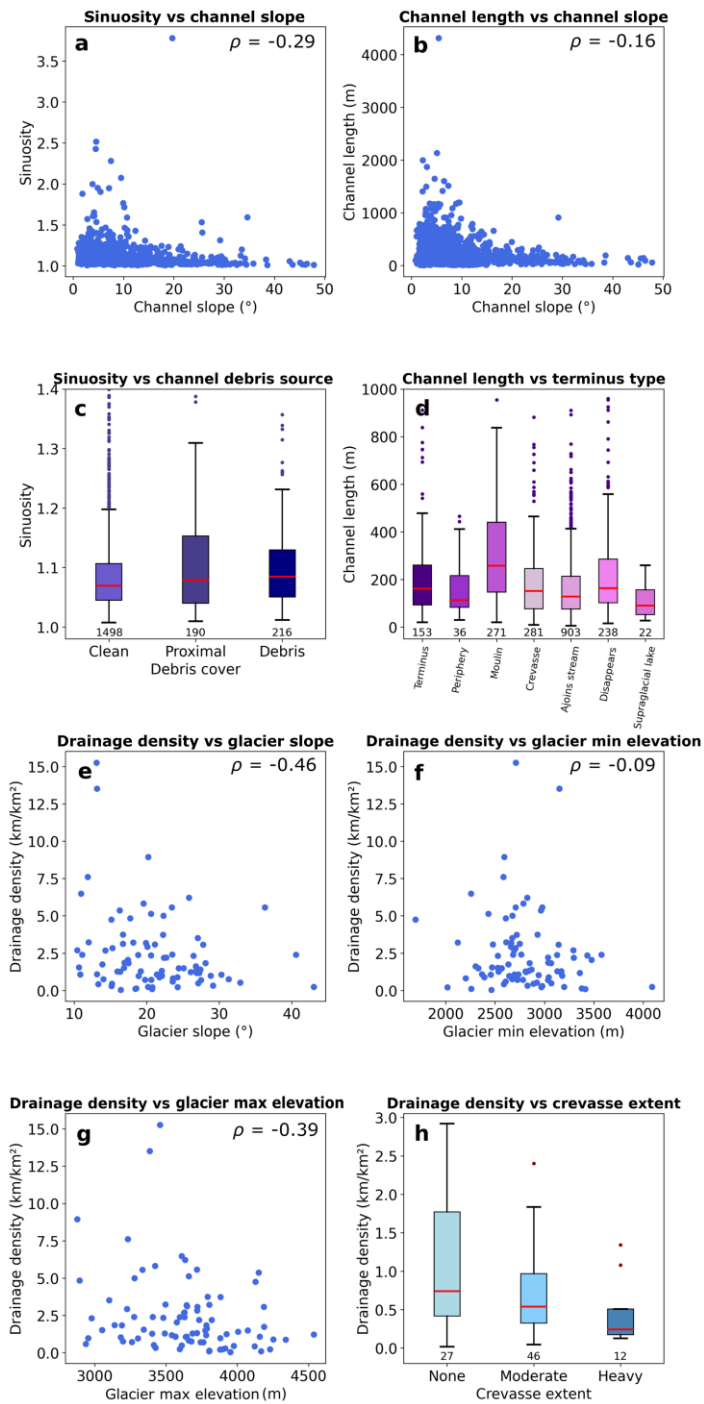


Figure 5: Relationships between channel characteristics (a-d) and glacier metrics (e-h). Plots a-d contain data from 1890 channels, and plots e-h contain data for the 85 glaciers with visible channels. Spearman's rank (ρ) values are included for all scatterplots, each of which is statistically significant ($p < 0.05$). (a) Sinuosity vs channel slope ($^{\circ}$); (b) channel segment length (m) vs channel slope ($^{\circ}$); (c) sinuosity vs channel debris source; (d) channel segment length (m) vs **channel terminus type; (e) drainage density (km/km^2) vs glacier slope ($^{\circ}$); (f) drainage density (km/km^2) vs minimum glacier elevation; (g) drainage density (km/km^2) vs maximum glacier elevation; and (h) drainage density (km/km^2) vs crevasse extent.**

Relationships between glacier metrics (Fig. 5e-h) are less clear than for channel characteristics (Fig. 5a-d), which may be due to the lower number of data points (85 glaciers compared to 1890 channels). However, a moderate negative correlation between drainage density and glacier slope exists, with the highest drainage densities occurring on the lowest surface slopes (Fig. 5e). A relationship between drainage density and minimum glacier elevation is less obvious (Fig. 5f), but there appears to be a peak in drainage density between 2600 and 3100 m a.s.l., which would require further validation from a larger sample of glaciers. By comparison, there is less evidence of a relationship between glacier drainage density and maximum glacier elevation (Fig. 5g). Likewise, there is no statistically significant relationship between glacier aspect and drainage density (Kruskal-Wallis test: $p = 0.61$). Glacier drainage density also tends to be higher on glaciers containing fewer crevasses (Fig. 5h).

4.4 Spearman's rank and Principal Component Analysis

We examined ~~the controls on~~ associations between channel morphometry and drainage density by calculating a correlation matrix. We use Spearman's rank correlation (ρ) and significance values (p), as many of our relationships are not linear. Given our large dataset and the fact that most p-values are < 0.05 , even modest correlations are statistically significant and likely reflect genuine relationships.

The strongest ~~control on~~ association with glacier drainage density is glacier mean elevation ($\rho = -0.66, p \leq 0.001$), with **relatively** higher drainage densities observed when a larger portion of **the** glacier area exists at lower elevations (Fig. 6), followed by glacier mean slope ($\rho = -0.46, p \leq 0.001$). This is consistent with Figure 5e, where the highest drainage densities are observed at glaciers with very low slope angles (e.g., Oberer Theodulgletscher; Fig. 4a).

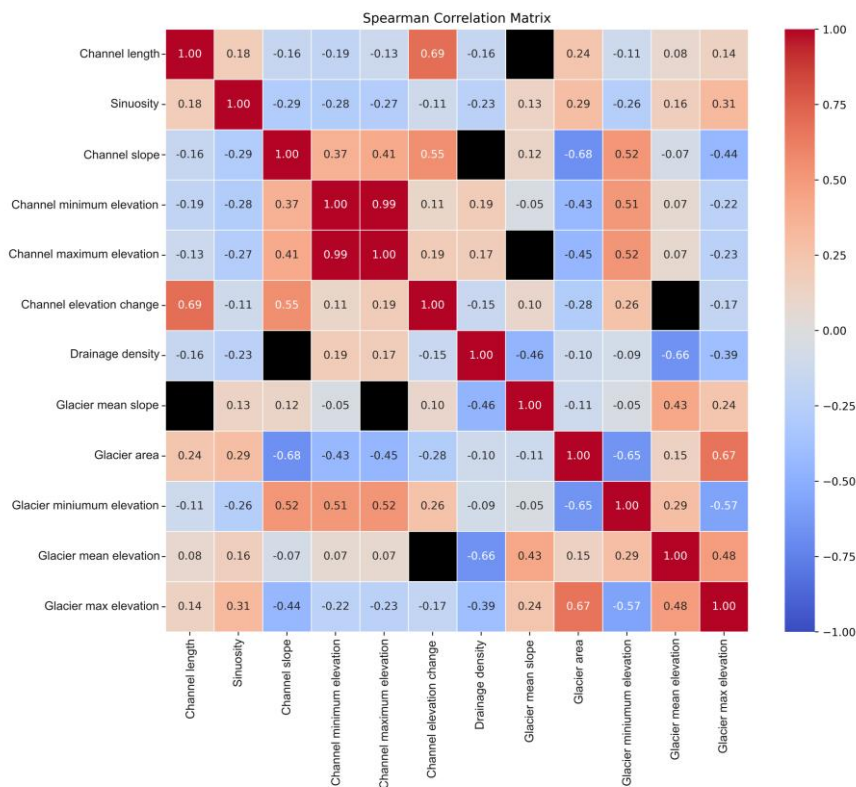


Figure 6: A heatmap matrix of Spearman's rank correlation showing the relationship between glacier and channel characteristics. Correlation values are scaled along a colour ramp, and non-significant relationships ($p > 0.05$) are coloured black.

By comparison, channel morphometry is characterised by more complex and weaker relationships between variables. For example, high channel sinuosity ~~can in part be explained by~~ shows no strong correlation with other variables but does exhibit multiple weak correlations. These show that sinuosity values tend to increase with a decrease in channel slope ($\rho = -0.29, p \leq 0.001$), and the most sinuous channels occur on larger glaciers ($\rho = 0.29, p \leq 0.001$) with lower minimum elevations ($\rho = -0.26, p \leq 0.001$) (Fig. 6). Channel slope ~~is primarily controlled by~~ shows strong associations with glacier characteristics. Channels with higher slope channels mostly exist on smaller glaciers ($\rho = -0.68, p \leq 0.05$), which that terminate at higher elevations ($\rho = 0.52, p \leq 0.05$), meaning the steepest channels are likely found at high elevation cirques and hanging glaciers.

To assess the relationship between variables and determine the drivers of variance, we conducted a Principal Component Analysis (PCA) using all channel and glacier variables included in our correlation matrix (Fig. 6). The PCA loadings show that glacier area has a large negative loading on ~~principal-component~~Principal Component (PC) 1, closely followed by strong positive loadings from minimum glacier elevation and channel elevation (maximum and minimum) (Table A1). By comparison, ~~principal-component~~PC 2 shows a strong positive loading from drainage density, and large negative loadings from mean glacier slope and glacier mean elevation (Table A1). ~~The first two components explain 50%~~ PC 1 explains 32% of the variance within the dataset, followed by PC 2 with an additional 13%, 12% and 9% explained by principal components 3, 4, and 18%. Together, PCs 1–5, respectively, which together explain 84% of the variabilityvariance (Table A1). Given the complexity of the dataset, our analysis using both channel and glacier variables reveals no clear visual clustering of data, but the PCA loadings show an expected relationship between elevation variables and slope variables. However, drainage density is not closely related to any other variable (Fig. A2). Overall, ~~our~~this PCA analysis reveals no single, primary driver of variance; instead, it is apparent that there is a complex, yet interlinked relationship between all variables that explain the distribution and appearance of supraglacial channels.

To further investigate how glacier characteristics affect the properties of channel networks (specifically drainage density and channel termini locations), we conducted an additional PCA and clustering analysis using only glacier characteristics found to have clear associations with drainage density (specifically slope and elevation) based on Spearman's rank correlation (Fig. 6). The clustering analysis revealed that glaciers with visible channels fall into three distinct classes: 51% are Type A, 43% are Type B, and 6% are Type C. Type A glaciers typically contain the steepest slopes (mean: 23.1°, terminate at high elevations (mean: 2,810 m a.s.l.), and have the lowest drainage density in our dataset (mean: 1.8 km/km²) (Type A; Fig. 7). Most channels on these glaciers tend to run directly off the glacier terminus (mean: 95%). Type B glaciers are typically less steep (mean: 18.9°) and have a lower minimum elevation (mean: 2774 m a.s.l.) than Type A glaciers, along with a slightly higher drainage density (mean: 2.2 km/km²) (Type B; Fig. 7). Most channels on Type B glaciers terminate englacially (87%), although a small percentage run off at the glacier terminus (13%). The few glaciers that are classified as Type C have the lowest minimum elevation (mean: 2659 m a.s.l.) and slope (mean: 15.5) in the dataset, and the highest drainage density (mean: 10.4 km/km²) (Type C; Fig. 7). At Type C glaciers, the number of channels that run off at the terminus (49%) and terminate englacially (51%) tends to be similar.

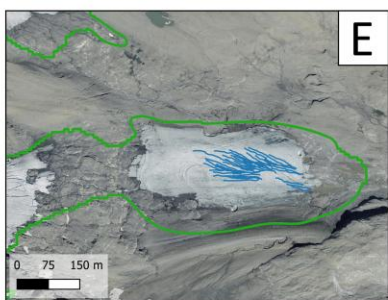
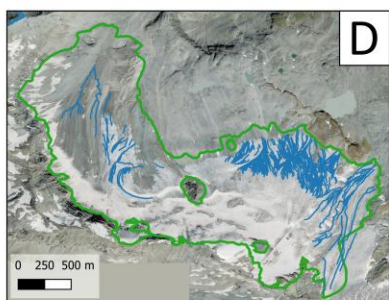
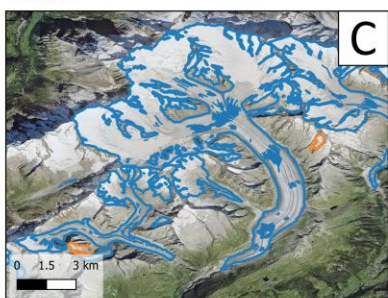
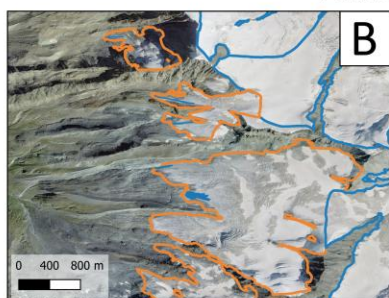
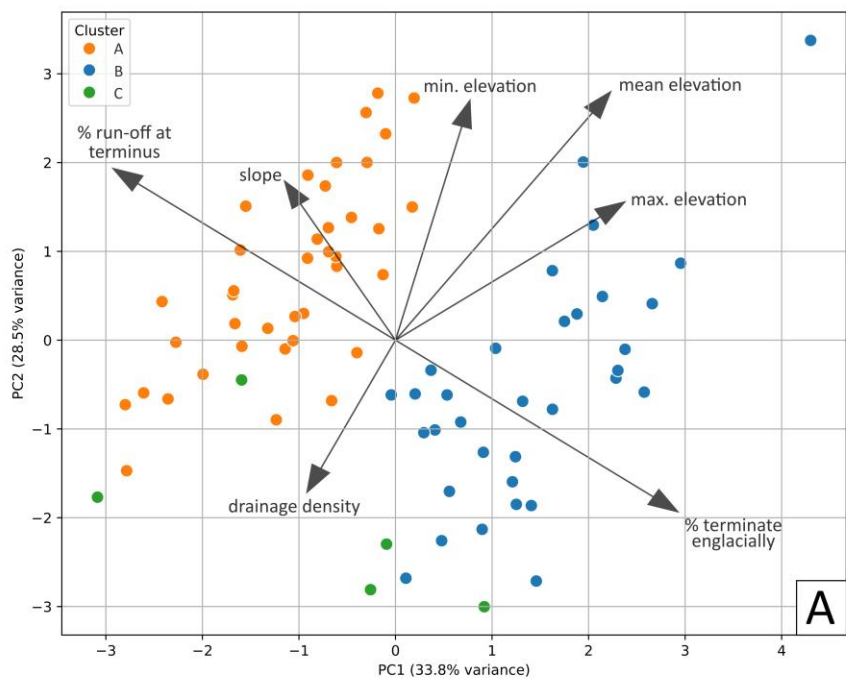


Figure 7. Glacier types across Valais categorised according to their terminus locations and characteristics. (A) A principal component analysis biplot of glacier characteristics overlaid with a loading plot. Each point is coloured based on its respective cluster (B). A group of type A glaciers, the largest being Mellichgletscher (centre right). (C) Several type B glaciers, e.g., Grosser Aletschgletscher (center right) and Oberaletschgletscher (far left). (D) An example of a Type C glacier - the Oberer Theodulgletscher. (E) A disconnection that has occurred from the main part of Wildstrubelgletscher. Both parts of the glacier are still treated as one connected mass based on the glacier outlines used, and are classified as Type C.

5 Discussion

5.1 The influence of glacier characteristics on supraglacial channel networks

Of the 285 glaciers in our study area, 85 contained channels (> 0.5 m) visible in high-resolution imagery (0.1 m) from August/September 2020. All of the largest glaciers (> 8 km²) contained visible channels (Fig. 3a), yet there was no clear relationship between glacier size and drainage density (Fig. 6). Instead, we find that drainage density has the strongest associations with glacier elevation (mean and maximum) and mean slope (Fig. 6). Our PCA (PC2; see Table A1 and Fig. A1) further revealed that higher drainage densities (e.g. generally > 10 km/km²) are typically found on glaciers with lower mean elevations (e.g. ~ 3000 m a.s.l) and gentler slopes (mean: $\sim 15^\circ$). We interpret the influence of elevation on drainage density as reflecting its control on surface melt rates, with lower-elevation glaciers more likely to support channel development because higher meltwater production is available for widespread channel incision. However, glaciers with a high meltwater supply may not have a high drainage density if the majority of meltwater is intercepted by crevasses (Fig. 5h). This is supported by our finding of lower drainage densities (e.g., ~ 2 km/km²) on steeper glaciers (Fig. 6), as steeper slopes typically contain a higher density of crevasses (Jiskoot et al., 2017). In Valais, steep, high-elevation glaciers are typically the smallest glaciers in the region, in the range of 0.1 to 1 km² (mean slope: 24.6° , mean minimum elevation: 2962 m a.s.l.). These glaciers may contain channel networks below our mapping resolution as channels are likely to be wider where meltwater supply is greater; nevertheless, we suggest that their drainage densities are likely lower than those of other Valais glaciers as our results indicate that even on glaciers with visible channels, high mean elevation and steeper slopes are less favourable for channel formation (Fig. 6).

465 5.1 — Our dataset also reveals large inter-glacier variability in meltwater transport pathways. Most of
466 the channels terminate englacially (72%); however, this is not the case for all glaciers. This figure is
467 skewed by the fact that a few glaciers contain a large proportion of all mapped channels. The
468 percentage of channels terminating englacially differs significantly when calculated for each
469 individual glacier and averaged across the dataset, primarily because the largest glacier (Grosser
470 Aletschgletscher) contains only englacially terminating channels. For this ‘average’ glacier value,
471 approximately 80% of channels run directly off the glacier terminus, while the remaining 20%
472 terminate englacially. We also find that a large proportion of glaciers (48%) only contain channels
473 that run off directly at the glacier terminus, compared to just 3.5% of glaciers that only contain
474 englacially terminating channels. This inter-glacier variability in channel termini locations is best
475 explained by the range of glacier characteristics present in our dataset. We find that steep, high-
476 elevation glaciers are likely to exhibit the greatest proportion of channels that run directly off the
477 glacier (mean: 95%) (Type A; Fig. 7). These glaciers are often characterised by heavily crevassed
478 terrain at higher elevations, which appears to inhibit channel formation due to the high density of
479 crevasses intercepting meltwater before channelisation occurs. Where channels do form, they are
480 typically confined to the few lower-relief areas close to the terminus and tend to run directly off it
481 (e.g., Fig. 7B). In contrast, glaciers that largely contain channels that terminate englacially (mean:
482 87%) tend to have slightly lower relief slopes and terminate at a lower elevation (Type B; Fig. 7).
483 These glaciers often exhibit a valley glacier configuration and typically contain a combination of
484 heavily crevassed areas (e.g., icefalls) and lower relief zones (e.g., Fig. 7C). Therefore, it is likely
485 that only channels forming down-glacier of densely crevassed areas, or those not intercepted by
486 moulins, reach the glacier terminus. While less common in our dataset, glaciers characterised by
487 particularly shallow slopes (e.g. $\sim 15^\circ$) and low minimum elevations (e.g. ~ 2700 m) tend to exhibit a
488 more even balance between channel termini locations (mean: 49% run off at the glacier terminus,
489 51% terminate englacially) (Type C; Fig. 7). Controls on the spatial distribution of channels

Formatted: Font color: Text 1

Formatted: Font color: Text 1

Formatted: Font color: Text 1

490 Of the 285 glaciers in our study area, 85 contained channels (> 0.5 m) visible in high-resolution imagery (0.1 m)
491 from mid-July 2020. The presence of visible channels is primarily controlled by a combination of sufficient
492 meltwater supply and distance for meltwater to coalesce and incise. Hence, in Valais, channels are infrequently
493 detected on cirque glaciers due to their smaller snow-free area, steeper and often crevassed slopes, and limited
494 distance for meltwater to coalesce. These cirque glaciers may contain channels below our mapping resolution;
495 however, they cannot be reliably quantified as part of this study. Glaciers containing channels tend to be larger,
496 resulting in the production of more surface melt. We found that all glaciers in Valais larger than 5.6 km^2 supported
497 channels and that glacier area controls much of the variability within the dataset (Table A1), albeit with large
498 variation in drainage density. This variation is in part attributed to glacier slope, which, together with ice-flow
499 velocity, governs the crevassed area of a glacier. This crevassed zone, in turn, controls the area in which channels
500 can form. For example, when crevasses are open, they can intercept meltwater, inhibiting the formation of longer
501 channels. Conversely, closed crevasses can add small-scale variability to surface topography, routing meltwater
502 along crevasse traces. Channel formation is also governed by glacier hypsometry, with glaciers containing a larger
503 portion of their area at lower elevations more likely to have higher drainage densities due to a larger snow-free
504 area (Fig. 6). We assume that our images from mid-July do not capture the maximum channel extent on higher
505 elevation glaciers. However, regardless of the image acquisition date, channel density will likely remain highest
506 at lower elevations where surface melt is greater.

507 The schematic in Figure 7 depicts how glacier elevation and hypsometry are likely to influence the distribution
508 and density of supraglacial channels in alpine settings. The lowest drainage densities are predicted to occur on
509 smaller cirque glaciers due to their lower meltwater supply, restricted distance for meltwater to coalesce into

channels, and increased channel interception due to crevasses on often steeper slopes (Fig. 7A). Whilst we detect very few channels on cirques due to our imagery resolution, these glaciers likely still contain networks of smaller channels. By comparison, larger valley glaciers (e.g., Grosser Aletschgletscher) tend to exhibit moderate to high drainage densities because they produce high amounts of meltwater, but much of it may be intercepted by crevasses on steeper slopes, preventing or restricting large channel formation (Fig. 7B). We suggest that fewer crevasses may result in a larger proportion of channels reaching the terminus, but where crevasses do occur, they are more likely to intercept channels, as low relief, low elevation glaciers typically have a high drainage density.

The conceptual schematic presented in Figure 8 characterises glaciers in Valais into three distinct types based on our cluster analysis of glacier properties: Type A, B, and C (Fig. 7). Glacier drainage density is predicted to progressively increase from Type A to C, coinciding with a decrease in glacier slope and lower minimum elevation (Fig. 8). The proportion of meltwater entering englacially is also predicted to decrease from Type A to C, which we suggest is likely to produce distinctly different runoff hydrographs at each glacier type. At Type A glaciers, runoff in response to surface melt is likely characterised by a small, earlier peak from a few supraglacial channels (light blue shading in Fig. 8A). The glaciers with the highest drainage densities are likely to have a large snow-free area (high meltwater supply) and occur on lower slopes because fewer crevasses allow large drainage networks to become established (Fig. 6; Fig. 7C). One example of this configuration is the Oberer Theodulgletscher which has the highest drainage density among Valais glaciers (Fig. 4a). It is possible that its high drainage density is also due to its location on a high elevation plateau, because air temperatures are likely to be cooler than at the termini of neighbouring glaciers which extend further down valley (Fig. 5f). As a result, the rate of surface lowering is likely slower, meaning that lower rates of incision are needed for channel formation to keep pace with surface lowering, resulting in a higher drainage density (Pitcher and Smith, 2019). However, summer temperatures in the Alps are increasing (Sommer et al., 2020), which will result in higher rates of surface lowering, meaning that all glaciers, but more specifically those with larger portions of their area at lower elevations, will require increased channel incision to counteract the higher rates of surface lowering (Marston, 1983).

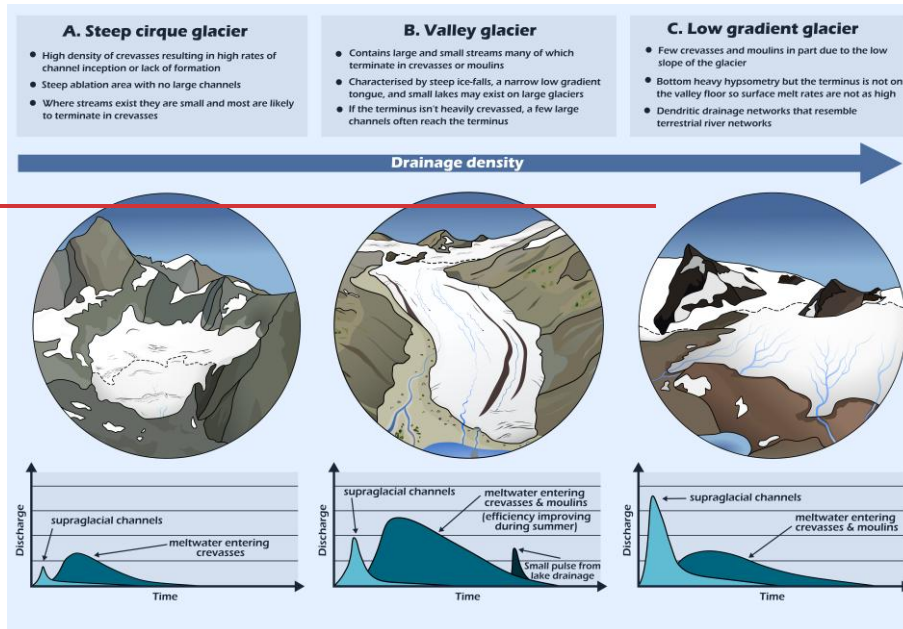


Figure 7: A schematic depicting the range of glacier types (A-C) and their respective characteristics, increasing in drainage density from left to right. Each glacier type corresponds to a hypothesised hydrograph (bottom) depicting changes in proglacial channel discharge over an unknown time period (ranging from minutes to days) as a response to a surface melt event. The hydrographs are hypothesised to represent the general characteristics of each glacier's runoff regime (see text for discussion) and do not reflect the complexities of individual measured proglacial stream discharge. Light blue shading shows the hypothesised hydrograph if all the meltwater were to be transported via supraglacial channels, whereas those shown in medium blue show the hydrograph where the bulk of meltwater is transported englacially/subglacially. Dark blue in panel (b) shows a lake drainage event.

The distribution and density of channels on different types of glaciers will likely impact the runoff hydrograph (Fig. 7). At small cirque glaciers, runoff in response to surface melt is likely characterised by a small earlier peak from a few supraglacial channels (light blue shading in Fig. 7A) or a slightly delayed peak as crevasses capture meltwater and route it through the en- (and -sub) glacial drainage systems (medium blue shading in Fig. 7A8A) (e.g., Clason et al., 2015). By comparison, valley Type B glaciers are larger and tend to contain more supraglacial channels, but, however, these channels are often intercepted by crevassed zones or ice falls/icefalls. This may result in an initial peak in meltwater from supraglacial the few channels that run-off directly at the terminus, followed by a delay in higher peak associated with meltwater that is routed en- (and sub-) glacially (Fig. 7B8B). Over the melt season, the lag time between melt/meltwater production and peak proglacial discharge typically decreases due to increased subglacial drainage network efficiency (Nienow et al., 1998). Additionally, some larger

valley Type B glaciers contain small supraglacial and ice marginal lakes (e.g., Gornergletscher and Grosser Aletschgletscher), which may experience infrequent drainage events (e.g., Huss et al., 2007), leading to a sudden peak in proglacial river discharge. Whilst less common in Valais, Type C glaciers are characterised by large shallow sloping areas that often contain extensive supraglacial drainage networks that capture the majority of surface melt (Fig. 7C8C). This is because shallow slopes typically have smaller and fewer crevasses than most valley glaciers. They will tend to have the 'flashiest' hydrograph because the supraglacial drainage network rapidly transfers melt off the glacier surface. Interception of this drainage by crevasses or moulins will increase the lag and decrease the amplitude of the hydrograph response. ▲

Formatted: Font color: Auto

Our dataset provides new insight into supraglacial channel distribution across a large range of glaciers, allowing simple inferences to be made about connectivity and possible lag times between melt and peak proglacial discharge based on the locations of our mapped channel termini. Overall, we find that at the average Valais glacier, 80% of channels run directly off the glacier, while the remaining 20% terminate in moulins or crevasses. However, this varies between glaciers and in the case of the largest glacier, Grosser Aletschgletscher (type B in Fig. 7), no mapped channels reach the terminus because of highly crevassed zones forcing meltwater into the glacier (53 % of channels enter moulins and 36 % enter crevasses). Unlike most glaciers in the Alps, small supraglacial lakes are also present on the Grosser Aletschgletscher, which capture 11 % of its channels. By comparison, the Oberer Theodulgletscher (type C in Fig. 7), which exhibits the highest drainage density, contains almost no moulins (2.8 % of channel termination), and 27 % of channels reach the terminus or periphery. A large number of channels terminate in crevasses on the Oberer Theodulgletscher (70 %), but crevasses tend to be small (<0.3 m wide), and it is not known whether meltwater enters englacially or is routed on the glacier surface through trace crevasses (e.g., Fig. 8). Observations have shown that trace crevasses may act as a preferential meltwater pathway, often resulting in channels forming perpendicular to ice flow (e.g., Chen et al., 2024). However, crevasses may also fill with meltwater and be continually overtopped if a channel is situated in a compressive regime, and thus less prone to hydrofracture (e.g., Chudley et al., 2021). As the true location of channel termination is unknown, our channel segments are always broken at crevasses if a clear pathway cannot be identified.

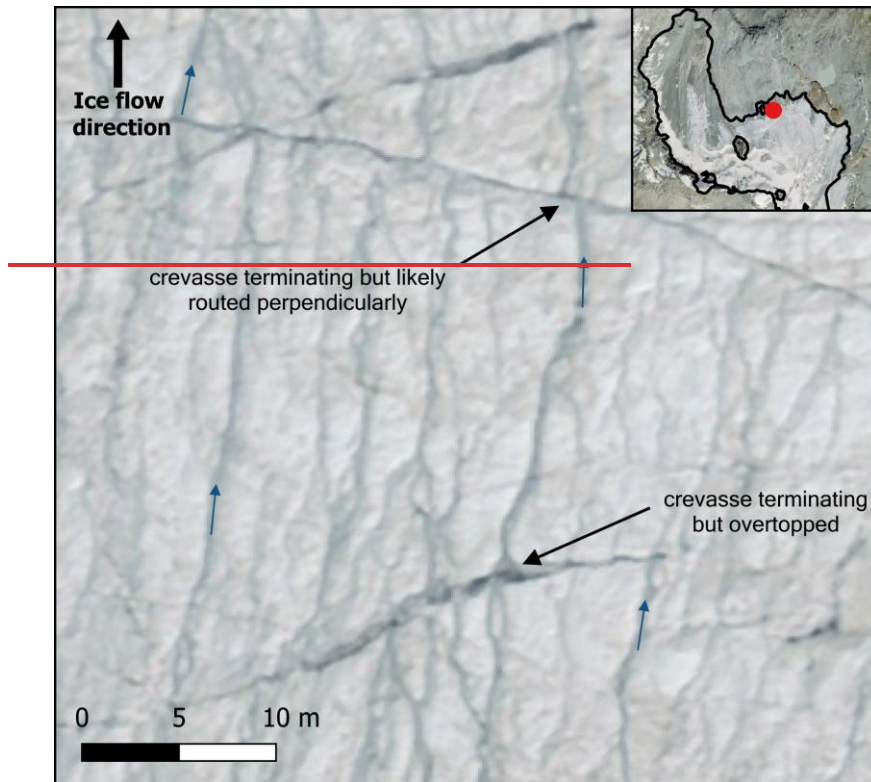
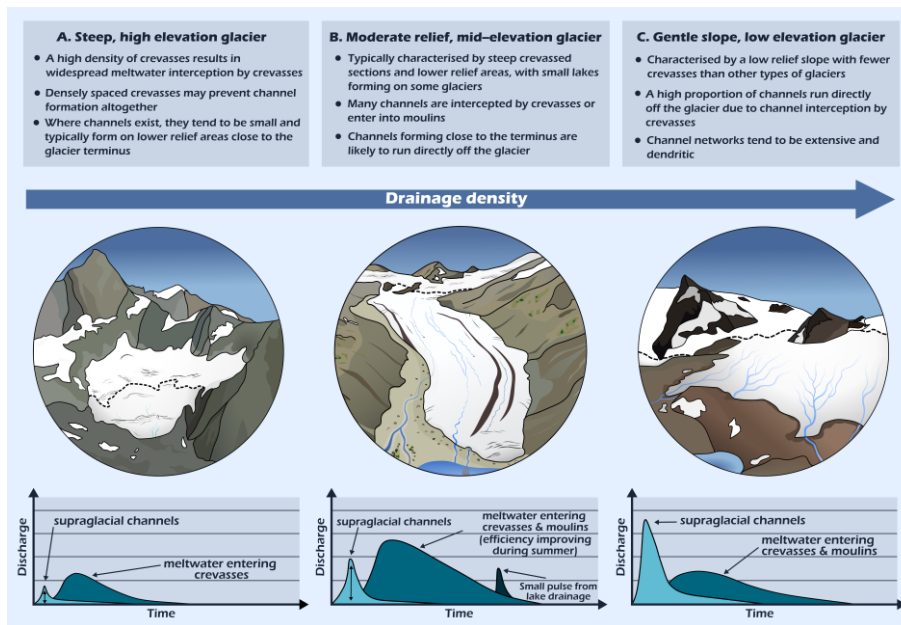


Figure 8: Examples of channels terminating in crevasses on the Oberer Theodulgletscher. The location of the main panel is shown in red on the glacier (top right). Channels are shown to terminate in crevasses but often continue directly down glacier as some meltwater overtops the crevasse. Small blue arrows indicate the direction of meltwater flow, with meltwater broadly flowing from the bottom to the top of the image. Imagery source: Federal Office of Topography Swisstopo.

The difference in drainage pathways between the Oberer Theodulgletscher and the Grosser Aletschgletscher can be explained by the difference in glacier type outlined in Figure 7. At the Grosser Aletschgletscher, increased meltwater capture by crevasses and moulins likely facilitates increased surface to bed meltwater transfer, which is supported by observations of its summer speed-up in ice flow velocity (Leinss and Bernhard, 2021). Model simulations suggest that increased meltwater presence at the glacier bed increases the excavation of subglacial sediment (Delaney and Adhikari, 2020), which would



598

Figure 8: A schematic depicting the range of glacier types (A-C) and their respective characteristics, increasing in drainage density from left to right. Each glacier type corresponds to a hypothesised hydrograph (bottom) depicting changes in proglacial channel discharge over an unknown time period (ranging from minutes to days) as a response to a surface melt event. The hydrographs are hypothesised to represent the general characteristics of each glacier's runoff regime (see text for discussion) and do not reflect the complexities of individual measured proglacial stream discharge. Light blue shading shows the hypothesised hydrograph if all the meltwater were to be transported via supraglacial channels, whereas those shown in medium blue show the hydrograph where the bulk of meltwater is transported englacially/subglacially. Dark blue in panel (b) shows a lake drainage event.

608

We also suggest that categorising glaciers based on their characteristics may allow for first-order predictions to be made about the extent of surface-to-bed meltwater transfer and relative proglacial stream sediment concentrations. For example, glaciers that contain the highest proportion of channels that terminate englacially, i.e., Type B glaciers, are likely to have a higher proportion of surface melt reaching the glacier bed. This may have implications for ice dynamics. Observations of seasonal speed-ups in ice flow velocity at the Grosser Aletschgletscher (Type B; Leinss and Bernhard, 2021), for example, may be more pronounced because all its mapped channels terminate englacially. Additionally, increased meltwater presence at the glacier bed has also been linked to higher rates of subglacial sediment excavation based on model simulations (Delaney and Adhikari,

2020). If subglacial till is present, this could result in higher proglacial stream sediment concentrations if streams are not diluted by freshwater flux from proglacially terminating supraglacial channels. This is important for In regions such as the Alps, this is important because proglacial stream sediment concentrations can directly impact agriculture and hydropower infrastructure (Micheletti and Lane, 2016). Hence, categorising glaciers based on their slope and hypsometry is beneficial because it provides insight into the anticipated drainage density of a glacier, probable channel pathways (i.e., sub-/englacially or proglacially terminating), and whether a higher amount of surface-to-bed meltwater transfer is likely.

Formatted: Font color: Text 1

Formatted: Highlight

5.2 ~~Controls~~Potential controls on channel morphometry

In Valais, there is a large variation in sinuosity values, with sinuous channels (1.05 - 1.25) occurring on some glaciers but not others. We find ~~that a~~ clear negative association between channel slope ~~affects~~and sinuosity, with the most sinuous channels (2.5 - 1.5) ~~likely tending to occur on lower angle slopes have a low slope~~ (0 to 10°) (Fig. 5a; Fig. 6; Table A2); in contrast, ~~steeper~~ channels ~~on steeper slopes~~ (> 20°) typically do not exhibit a sinuosity over 1.3. ~~Channels tend to be~~This aligns with observations of fluvial systems, where rivers on steeper terrain tend to be less sinuous and have a narrower range of sinuosity values (Schumm, 1963; Frasson et al., 2019). The exact cause and mechanisms of meander formation are still disputed in fluvial systems (Finotello et al., 2024); however, many of these explanations focus on sediment transport (Rhoads and Welford, 1991). While it is apparent that sinuous supraglacial channels can form on areas with and without high volumes of sediment (e.g., Fig. 4d-e), we find some distinct differences in sinuosity between channels with differing proximity to debris. For example, channels are typically least sinuous on debris-free ice, slightly more sinuous on thicker debris cover, and the most sinuous on moderately debris-covered ice (Fig. 5e). ~~However, the most sinuous channels are found on predominantly debris-free ice on Gornergletscher (Fig. 4e). The high prevalence of sinuous channels on moderately~~5c). It is likely that channels on or close to ~~debris-covered ice may be due to~~ sources contain sediment, which may amplify channel sinuosity, as supported by previous findings of increased sediment in the channels, ~~sourced from the surrounding terrain, which was also found to increase channel sinuosity at transport producing higher sinuosity channels on an Alaskan glacier (Boyd et al., 2004). However, the~~2024). However, further research is required to better understand the impact of sediment in supraglacial channels on channel properties, as this remains poorly understood. We also find that the relationship we observe between slope and channel sinuosity in Valais (Fig. 5a) differs from ~~the~~our study contrasts with findings ~~off~~from a High Arctic glacier. St. Germain and Moorman (2019), who found that channels on a High Arctic glacier were more sinuous on steeper slopes. This difference may be explained by three factors. The first is that channel distribution in Valais is heavily influenced by crevassed areas (Fig. 5b; Fig. 6), meaning that channel formation is more likely on flatter areas with fewer crevasses. A second consideration is channel discharge, which we do not measure here. Discharge and slope control stream power, which has been found to positively correlate with sinuosity (Ferguson et al., 1973; Marston, 1983; St Germain and Moorman, 2019). We cannot separate out the relative impacts of slope and discharge. However, higher discharges are most likely to form on flatter areas with fewer crevasses, as they favour the development of longer channels-) reported a positive relationship, suggesting that sinuosity increases with slope. In contrast, our observations indicate that sinuosity typically increases as slope decreases (Fig. 5a). Given the

655 large number of channels we delineated, we are confident that we have reliably captured the relationships among
656 variables in our dataset. We suggest that this discrepancy may be due to differences (e.g., Fig. 5b). Additionally,
657 reduced meltwater interception in flatter areas allows more meltwater to enter channels, potentially increasing
658 sinuosity. Finally, the sediment cover of many glaciers in Valais exceeds that of the glacier examined by St
659 Germain and Moorman (2019). Hence, channel sediment content is likely higher in Valais, which may increase
660 channel sinuosity due to enhanced erosion during sediment transport or, alternatively, reduce erosion where the
661 bed is covered by thick sediment. Overall, the difference in relationship between slope and sinuosity between
662 Valais and a glacier High Arctic is attributed to the effect of multiple independent variables on sinuosity, which
663 differ in impact between locations, sample size or environmental conditions.

Formatted: Font color: Text 1

Formatted: Not Highlight

Formatted: Font color: Auto

665 5.3 Comparison between Valais glaciers and the Greenland Ice Sheet

666 Previous research on supraglacial channel morphometry networks has predominantly focused on the GrIS (e.g.,
667 Smith et al., 2015; Karlstrom and Yang, 2016; Yang and Smith, 2016; Yang et al., 2016, 2021, 2022), with). We
668 find some similarities in drainage patterns observed between the GrIS and Valais glaciers, and the Greenland Ice
669 Sheet (GrIS). For example, in Valais, larger glaciers often contain both environments show a negative correlation
670 between drainage density and mean elevation (Yang et al., 2016), although this correlation is more pronounced
671 on Valais glaciers (Fig. 6). Channel networks also appear to exhibit visually similar drainage patterns. In Valais,
672 many glaciers exhibit dendritic drainage patterns (e.g., 4a), which are commonly observed on similar to the GrIS
673 (e.g., Yang et al., 2016, 2019). However, some glaciers in Valais display parallel, weakly interconnected channel
674 networks, likely due to insufficient distance for meltwater to converge into a single channel. It could be expected
675 that, given sufficient distance for meltwater to coalesce, these networks would be comparable to networks drainage
676 patterns observed on the southwest GrIS, which were found to broadly follow Horton's laws, i.e., mean river
677 length increases with channel order and mean slope decreases with channel order (Yang et al., 2016). On a smaller
678 scale, ice surface structures (e.g., trace crevasses) exhibit a strong control on meltwater routing on Valais glaciers
679 and on both the Greenland and Antarctic ice sheets (e.g., Fig. 4e; Chen et al., 2024). However, Valais also contains
680 some more parallel weakly interconnected channel networks (e.g., Fig. 4f). Where parallel channel networks occur
681 on the GrIS, particularly in regions such as Inglefield Land, they tend to be long (<55 km), straight, and are
682 typically found in areas with minimal elevation change and slow ice flow, unlike dendritic channels on the
683 southwest GrIS, which occur on more undulating topography (Yang et al., 2019). Like the GrIS, the range of
684 drainage patterns on Valais glaciers may relate to variations in glacier surface topography. However, it is not
685 known whether parallel networks on Valais glaciers simply occur due to constraints on channel length and density
686 (i.e., glacier area, high crevasse density) (Fig. 5h; Fig. 6), or whether, given sufficient distance, these channels
687 would have coalesced to form dendritic patterns.

Formatted: Font color: Auto

Formatted: Font color: Auto

688 Nevertheless, We also find large inter-glacier variability in channel termini locations between Valais and glaciers,
689 whereas this appears to be more regionally consistent on the GrIS differ in where (Yang et al., 2019). In Valais,
690 distinct glacier types tend to be characterised by different proportions of channel termini locations (i.e., englacially
691 terminating vs running off at the terminus) (Fig. 7; Fig. 8). Hence, the extent of surface-to-bed connections likely
692 varies amongst the Valais dataset, particularly as some glaciers only support englacially-terminating channels

Formatted: Font color: Auto

693 terminate, and their glacier surface characteristics are often dissimilar (e.g., debris coverage). On (3.5%) or
 694 channels that all run off the glacier (48%). By comparison, on the southwest GrIS, virtually all higher-order
 695 channels terminate in moulins (Smith et al., 2015), whereas at the average Valais glacier, only 20 % of our mapped
 696 channels terminate englacially. This suggests notable differences in coupling between surface channels and the
 697 englacial/subglacial system. There is also a general absence of supraglacial lakes in Valais, also exist
 698 in abundance on the GrIS, providing potential for interannual storage and rapid meltwater drainage to the bed
 699 (Chu, 2014). Given few channels in Valais terminate in lakes (Fig. 5d), except for small lakes on Gornergletscher
 700 and the Grosser Aletschgletscher, meaning few channels terminate in lakes, whereas lakes exist in abundance on
 701 the GrIS (Chu, 2014). Additionally, (e.g., Fig. 4e), it is likely that proglacial stream discharge here is more closely
 702 linked to surface melt and rainfall.

703 More extensive debris cover on Valais glaciers compared to the GrIS could also result in differences in channel
 704 morphology and distribution. For instance, we find that more sinuous channels often occur close to debris cover
 705 is more extensive in Valais and accumulations (see Section 5.2), which may suggest that channel sinuosity is
 706 observed to, in part, modulated by its sediment content. Widespread debris cover will also affect channel
 707 morphology (see section 5.2) and distribution. The latter is evident from the formation surface topography. For
 708 example, larger-scale features (e.g., medial and lateral moraines) may influence meltwater transport by restricting
 709 the pathways for meltwater runoff. It might also be expected that the topographic depressions that typically occur
 710 at this ice-debris interface influence the accumulation of high amounts of meltwater. Therefore, large channels
 711 may be expected to disproportionately form parallel to lateral or medial moraines due to topographic confinement
 712 (e.g., Fig. 4b). Debris cover also modulates surface melt and influences both micro-scale and larger-scale. On a
 713 smaller scale, the presence of debris may notably affect surface roughness, which in some cases has been
 714 associated with increased higher channel density densities (Rippin et al., 2015). However, whilst the scale of
 715 sediment coverage differs, debris may play a significant role in controlling channel distribution and
 716 morphology, particularly in mountainous regions where debris is more abundant than in ice sheet settings.
 717 Nevertheless, even on the GrIS, where debris cover is comparatively limited, the presence of dust, black carbon,
 718 algae, and cryoconite deposits on the GrIS may still affect exert an influence on channel distribution and
 719 morphometry (e.g., Ryan et al., 2018; Leidman et al., 2021; Khan et al., 2023).

721 5.4 Future Outlook and future evolution of supraglacial channel systems

722 The impact of climatic warming on supraglacial drainage networks is not fully understood, but we suggest previous
 723 research on ice sheets suggests that supraglacial drainage networks may expand are likely to continue expanding
 724 to higher elevations due to rising equilibrium lines (Leeson et al., 2015). Whether discharge in current channels
 725 will increase increases or decrease decreases depends on the rates of glacier retreat and surface lowering, driven by
 726 ablation. It is likely that larger glaciers will see an increase in channel discharge due to rising equilibrium lines
 727 and associated higher rates of surface melt (St Germain and Moorman, 2019). However, the reduction in area for
 728 smaller glaciers may be large enough sufficient to prevent the formation of efficient drainage networks. Changes
 729 in glacier slope could also result in a reconfiguration of the drainage system (e.g., new crevasses may intercept
 730 channels that formerly reached the terminus), which may affect drainage density (Fig. 5e): glacier terminus), which

Formatted: Font color: Auto

Formatted: Font color: Auto

Formatted: Font color: Auto

Formatted: Font color: Auto

Formatted: Font color: Auto

Formatted: Font color: Auto

Formatted: Font color: Auto

Formatted: Font color: Auto

Formatted: Font color: Auto

Formatted: Font color: Auto

Formatted: Font color: Auto

Formatted: Font color: Auto

Formatted: Font color: Auto

Formatted: Font color: Auto

Formatted: Font color: Auto

Formatted: Font color: Auto

Formatted: Font color: Auto

Formatted: Font color: Auto

Formatted: Font color: Auto

may affect drainage density (Fig. 5e). This may also result in increased disconnections (i.e., separation of the accumulation and ablation area), as observed at a Type C glacier (Fig. 7E). Such disconnections (see Davies et al., 2024) may result in high channel densities on the isolated ice mass due to accelerated downwasting. Additionally, glaciers in some mountain environments are undergoing an increase in debris cover (e.g., Glasser et al., 2016; Fleischer et al., 2021), and it is not fully understood how changes in debris cover will affect surface meltwater supply and transport, channel morphometry and morphology, and surface albedo (e.g., Leidman et al., 2021).

Future research could benefit from utilising the growing repository of high-resolution orthophoto surveys to improve our understanding of supraglacial hydrology in mountain glacier settings. Increased understanding of seasonal and interannual channel evolution is needed to better inform modelling of glacier hydrology. For example, it is not clear whether our findings would also apply to regions with larger glaciers and lower rates of surface lowering (e.g., the Arctic), so future studies could repeat our work in such regions. Lastly, further in-situ measurements would be beneficial to determine whether the channels delineated as part of this study represent the majority of meltwater transport on Valais glaciers or whether channels below our mapping resolution also play a key role in meltwater transport.

6 — Conclusion

6 Conclusions

This study presents the first comprehensive dataset on the distribution and characteristics of supraglacial channels at a regional scale in a mountain glacier environment. ~~Out~~From a sample of 285 glaciers in Valais Canton, Switzerland, we identified 85 glaciers that contained channels above our mapping resolution (0.5 m wide). ~~We found substantial variability in glacier drainage density, with the highest values occurring on glaciers with shallow slopes and a large portion of their surface area at lower elevations (Fig. 7). We found that while glaciers containing visible channels have a larger mean area (5 km²) than those without (0.6 km²), glacier area alone is not a good predictor of drainage density. Rather, our findings suggest that variability in drainage density is most strongly controlled by glacier surface slope and mean elevation. These variables enabled the classification of glaciers in Valais into distinct types, each characterised by different drainage densities. Type A glaciers are characterised by both low mean elevations and low-angle slopes, and they exhibit the highest drainage densities, likely due to a greater meltwater supply and fewer crevasses, which can fragment channel networks or, when present at high densities, inhibit channel formation altogether. Type B glaciers are intermediate between Types A and C, the latter of which typically contain very few channels and are the steepest and highest-elevation glaciers in Valais 7). The presence of channels is primarily dictated by a sufficiently supply of meltwater (i.e., large enough glacier area) and an uninterrupted distance for meltwater to coalesce (i.e., absence of crevasses). The primary control on channel distribution is surface topography, with the slope and size of the snow-free area providing a clear limit on both where channels can form and their total length (Fig. 5b). However, strong structural controls on channel distribution exist. For example, trace crevasses have been observed to act as preferential meltwater pathways, resulting in channels forming perpendicular to ice flow. Channels also commonly form parallel to medial and~~

Formatted: Font color: Auto

Formatted: Font color: Auto

Formatted: Font color: Auto

Formatted: Font color: Text 1

lateral moraines due to topographic confinement. Most channels are characterised by low sinuosity (Fig. 5a), although some highly sinuous channels are present, particularly on moderately debris-covered ice and lower-relief glacier termini. This contrasts with cold or polythermal glaciers, where sinuous channels are more commonly found on steeper slopes. These findings suggest that controls on channel morphology and morphometry are not consistent across mountain glacier environments and may instead reflect variations in debris cover, the location and density of crevassed zones, and rates of surface lowering.

In Valais, most glaciers are characterised by a high proportion of channels that reach the glacier margin without being routed into the glacier. On average, approximately 80 % of channels per glacier run directly off the glacier (terminate proglacially), while the remaining 20 % terminate in a crevasse or moulin. We find that 48 % of glaciers support only proglacially terminating channels, whereas 3.5 % of glaciers are characterised by entirely englacially-terminating channels. The location of channel termini (i.e., proglacial or englacial) is hypothesized to produce different hydrograph responses to surface melt, some of which we suggest may be more common for certain glacier hypsometries (Fig. 6). There is also notable inter-glacier variability in the proportion of channels terminating englacially (i.e., in moulins or crevasses), which is also consistent with our glacier classification. The highest proportion of channels that run directly off the glacier is observed at steep, high-elevation glaciers. The few channels that are present tend to form close to the terminus on flatter, less crevassed terrain, meaning that almost all channels run off the terminus. In contrast, up-glacier, most meltwater is captured prior to channelisation due to densely spaced crevasses. Glaciers with moderate relief slopes and mid-range mean elevations tend to have the highest proportion of englacially terminating channels and typically have a moderate drainage density. Many of these channels are intercepted by crevassed zones before they reach the terminus. In contrast, low-relief, low-elevation glaciers display a mixture of channel termination types. These glaciers often have very high drainage densities, and, due to fewer crevasses, many channels run off the terminus. However, where crevasses are present, they are more likely to intercept channels. Consequently, hydrograph responses to surface melt and the extent of surface-to-bed connections are likely to vary between different glacier types. This contrasts with the Greenland Ice Sheet, where channels frequently terminate in lakes, which is uncommon in Valais. We also suggest that proglacial stream discharge in Valais likely exhibits a more immediate response to melt events, with reduced lag times due to minimal opportunity for supraglacial storage.

Lastly, we observe that channel and drainage network characteristics vary across our dataset. We find that higher channel sinuosities tend to occur on lower glacier surface slopes, consistent with observations from fluvial systems. Our findings also suggest that the transport of sediment into channels from nearby sources may increase sinuosity, although further research is needed to investigate the influence of debris cover on channel morphometry. The networks we observe commonly exhibit dendritic patterns, which closely resemble those on the southwest Greenland Ice Sheet that have been found to broadly follow Horton's Laws. Additionally, some less-connected channel networks are observed, which also occur on ice sheets. It is not known whether these less-connected networks form due to topographic controls, as in ice sheet settings, or whether they could become dendritic in the absence of controls on their length (i.e., glacier area or crevasse and moulin capture). Lastly, future research should investigate how drainage networks on rapidly thinning glaciers, such as those in the Alps, will evolve under climate warming, as alterations in glacier slope, elevation, and debris cover are likely to impact drainage density and the routing of meltwater.

Formatted: Font color: Auto

807
808
809
810
811
812
813
814
815
816
817
818
819
820
821
822
823
824
825
826
827
828

~~7) Channel terminus locations in Valais differ from those described in prior research, which has largely focused on the SW GrIS, where most channels terminate in moulins and very few reach the ice margin. Similar to the GrIS, drainage networks on Valais glaciers often exhibit dendritic patterns. However, such configurations are likely less widespread due to smaller drainage areas and limited distance for channels to merge.~~

Formatted: Font color: Text 1

Appendix A: Principal Component Analysis

Table A1: The eigenvectors for ~~principal components~~**Principal Components** 1 to 6 from a PCA analysis of glacier and channel characteristics, with ~~PC1~~**Principal Component 1** being the most significant. The three largest loadings for each principal component are in bold.

	PC1	PC2	PC3	PC4	PC5	PC6
Glacier area	-0.439	0.042	0.034	0.288	-0.187	0.054
Glacier minimum elevation	0.435	-0.112	0.085	-0.098	0.407	-0.178
Channel maximum elevation	0.393	0.159	0.066	0.436	-0.115	0.186
Channel length	-0.070	-0.264	-0.582	0.312	0.195	-0.199
Channel minimum elevation	0.382	0.196	0.121	0.423	-0.100	0.196
Channel sinuosity	-0.117	-0.182	-0.122	-0.041	0.468	0.845
Channel elevation range	0.166	-0.345	-0.542	0.198	-0.173	-0.068
Channel slope	0.320	-0.203	-0.066	-0.115	-0.483	0.255
Drainage density	0.131	0.543	-0.268	-0.009	0.041	0.083
Mean glacier slope	0.119	-0.439	0.136	-0.309	-0.335	0.141

Glacier mean elevation	0.170	-0.376	0.401	0.280	0.339	-0.188
Glacier max elevation	-0.330	-0.175	0.264	0.462	-0.163	0.086

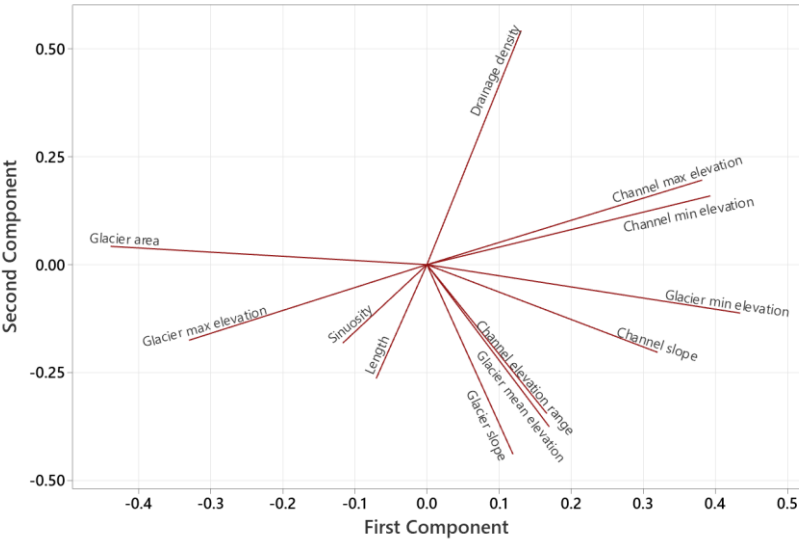


Figure A1: Loading plot for **principal-componentsPrincipal Components** 1 and 2 from a PCA analysis of glacier and channel characteristics.

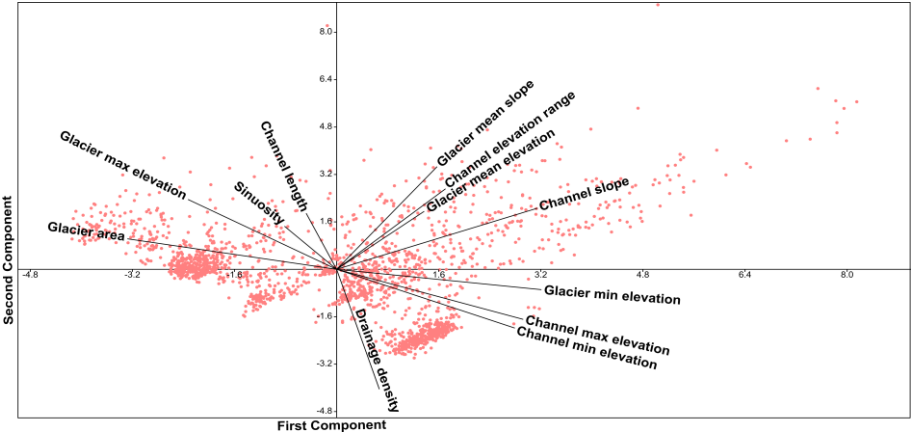


Figure A2: A biplot from a PCA analysis showing **principal-componentsPrincipal Components** 1 and 2, which were used for visually identifying clusters and overlayed with a loading plot (see Fig. A1).

Appendix B: Accuracy Assessment

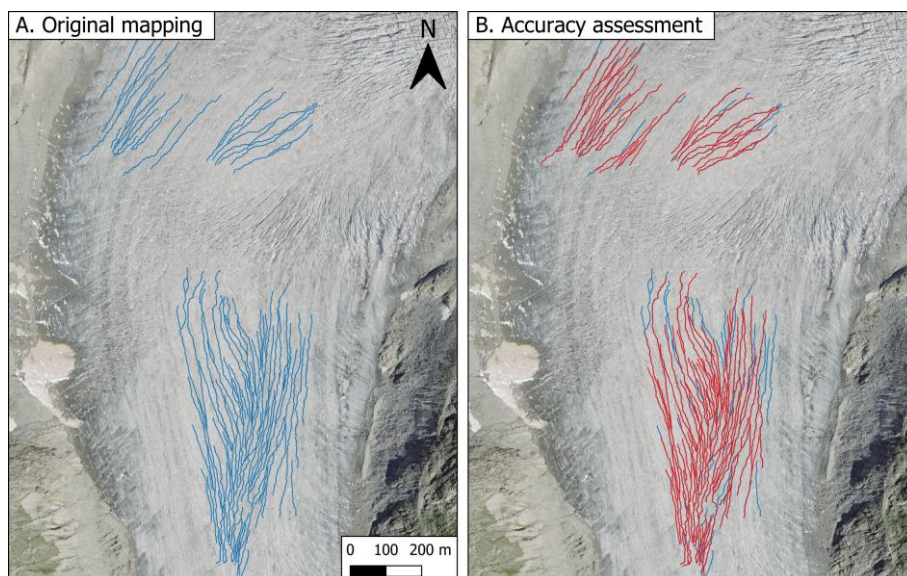


Figure B1: Repeat mapping of the Rhonegletscher used to determine mapping accuracy. (A) Mapping from this dataset is shown in blue. (B) A comparison between the repeat mapping (red) and the original mapping (blue) was undertaken independently after several weeks had elapsed.

Data availability

The orthophoto and DEM data used in this study are freely available on the SwissTopo website (<https://www.swisstopo.admin.ch/>). Outlines of glaciers in Valais were obtained from Glacier Monitoring in Switzerland (GLAMOS) and are available online (<https://glamos.ch/>). The produced supraglacial channel data is available upon request from the corresponding author (Holly Wytiahlowsky: holly.e.wytiahlowsky@durham.ac.uk).

Author contributions

All authors contributed to the conceptualisation of this project. HW conducted the mapping, analysis and data visualisation under the supervision of CRS, RAH, CCC and SSRJ. HW led manuscript writing with comments and edits provided by all authors.

Competing interests

CC is a member of the editorial board of The Cryosphere, and CRS was a member at the time of submission.

862 **Acknowledgements**

863 This work was supported by the Natural Environment Research Council via an IAPETUS2 PhD studentship held
864 by Holly Wytiahlowsky (grant reference NE/S007431/1). We thank SwissTopo for making their orthophotos and
865 DEM data open access. We thank two anonymous reviewers and Ian Willis for their constructive feedback, which
866 has helped to improve this paper, and Kang Yang for acting as editor for the manuscript.

867

868 **7 References**

- 869 Bamber, J. L., Oppenheimer, M., Kopp, R. E., Aspinall, W. P., and Cooke, R. M.: Ice sheet contributions to
870 future sea-level rise from structured expert judgment, *Proc. Natl. Acad. Sci.*, 116, 11195–11200,
871 doi:10.1073/pnas.1817205116, 2019.
- 872 Banwell, A., Hewitt, I., Willis, I., and Arnold, N.: Moulin density controls drainage development beneath the
873 Greenland ice sheet, *J. Geophys. Res. Earth Surf.*, 121, 2248–2269, doi:10.1002/2015JF003801, 2016.
- 874 Bell, R. E., Chu, W., Kingslake, J., Das, I., Tedesco, M., Tinto, K. J., Zappa, C. J., Frezzotti, M., Boghosian, A.,
875 and Lee, W. S.: Antarctic ice shelf potentially stabilized by export of meltwater in surface river, *Nature*, 544,
876 344–348, doi:10.1038/nature22048, 2017.
- 877 Brice, J. and Blodget, J.: Countermeasures for Hydraulic Problems at Bridges, Volume 1 – Analysis and
878 Assessment.
- 879 Boyd, B., Goetz, S. L., and Ham, N. R.: Supraglacial stream incision into debris-covered ice, Matanuska
880 Glacier, AK. *Geol. Soc. Am. Abstr.*, 36, 11.
- 881 Carey, M., Molden, O. C., Rasmussen, M. B., Jackson, M., Nolin, A. W., and Mark, B. G.: Impacts of glacier
882 recession and declining meltwater on mountain societies, *Ann. Am. Assoc. Geogr.*, 107, 350–359,
883 doi:10.1080/24694452.2016.1243039, 2017.
- 884 Chen, J., Hodge, R. A., Jamieson, S. S. R., and Stokes, C. R.: Distribution and morphometry of supraglacial
885 channel networks on Antarctic ice shelves. *J. Glaciol.*, doi:10.1017/jog.2024.99, 2024.
- 886 Chu, V. W.: Greenland Ice Sheet hydrology: A review, *Prog. Phys. Geogr.*, 38, 19–54,
887 doi:10.1177/0309133313507075, 2014.
- 888 ~~Chudley, T. R., Christoffersen, P., Doyle, S. H., Bougamont, M., Schoonman, C. M., Hubbard, B., and James,~~
889 ~~M. R.: Supraglacial lake drainage at a fast-flowing Greenlandic outlet glacier, *Proc. Natl. Acad. Sci.*, 116,~~
890 ~~25468–25477, doi:10.1073/pnas.1913685116, 2019.~~
- 891 ~~Chudley, T. R., Christoffersen, P., Doyle, S. H., Dowling, T. P. F., Law, R., Schoonman, C. M., Bougamont, M.,~~
892 ~~and Hubbard, B.: Controls on Water Storage and Drainage in Crevasses on the Greenland Ice Sheet, *J. Geophys.*~~
893 ~~*Res. Earth Surf.*, 126, e2021JF006287, doi:10.1029/2021JF006287, 2021.~~
- 894 Clason, C. C., Coch, C., Jarsjö, J., Brugger, K., Jansson, P., and Rosqvist, G.: Dye tracing to determine flow
895 properties of hydrocarbon-polluted Rabots glaciär, Kebnekaise, Sweden, *Hydrol. Earth Syst. Sci.*, 19, 2701–
896 2715, doi:10.5194/hess-19-2701-2015, 2015.
- 897 Clason, C. C., Rangecroft, S., Owens, P. N., Łokas, E., Baccolo, G., Selmes, N., Beard, D., Kitch, J., Dextre, R.
898 M., Morera, S., and Blake, W.: Contribution of glaciers to water, energy and food security in mountain regions:
899 current perspectives and future priorities, *Ann. Glaciol.*, 63, 73–78, doi:10.1017/aog.2023.14, 2023.
- 900 Davaze, L., Rabatel, A., Dufour, A., Hugonnet, R., and Arnaud, Y.: Region-wide annual glacier surface mass
901 balance for the European Alps from 2000 to 2016, *Front. Earth Sci.*, 8, doi:10.3389/feart.2020.00149, 2020.

902 [Davies, B., McNabb, R., Bendle, J., Carrivick, J., Ely, J., Holt, T., Markle, B., McNeil, C., Nicholson, L., and](#)
903 [Pelto, M.: Accelerating glacier volume loss on Juneau Icefield driven by hypsometry and melt-accelerating](#)
904 [feedbacks, *Nat. Commun.*, 15, 5099, doi: 10.1038/s41467-024-49269-y, 2024.](#)

905 Delaney, I. and Adhikari, S.: Increased subglacial sediment discharge in a warming climate: consideration of ice
906 dynamics, glacial erosion, and fluvial sediment transport, *Geophys. Res. Lett.*, 47, e2019GL085672,
907 doi:10.1029/2019GL085672, 2020.

908 Dozier, J.: An examination of the variance minimization tendencies of a supraglacial stream, *J. Hydrol.*, 31,
909 359–380, doi:10.1016/0022-1694(76)90134-7, 1976.

910 Edwards, T. L., Nowicki, S., Marzeion, B., Hock, R., Goelzer, H., Seroussi, H., Jourdain, N. C., Slater, D. A.,
911 Turner, F. E., Smith, C. J., McKenna, C. M., Simon, E., Abe-Ouchi, A., Gregory, J. M., Larour, E., Lipscomb, W.
912 H., Payne, A. J., Shepherd, A., Agosta, C., Alexander, P., Albrecht, T., Anderson, B., Asay-Davis, X.,
913 Aschwanden, A., Barthel, A., Bliss, A., Calov, R., Chambers, C., Champollion, N., Choi, Y., Cullather, R.,
914 Cuzzzone, J., Dumas, C., Felikson, D., Fettweis, X., Fujita, K., Galton-Fenzi, B. K., Gladstone, R., Golledge, N.
915 R., Greve, R., Hattermann, T., Hoffman, M. J., Humbert, A., Huss, M., Huybrechts, P., Immerzeel, W., Kleiner,
916 T., Kraaijenbrink, P., Le clec'h, S., Lee, V., Leguy, G. R., Little, C. M., Lowry, D. P., Malles, J.-H., Martin, D. F.,
917 Maussion, F., Morlighem, M., O'Neill, J. F., Nias, I., Pattyn, F., Pelle, T., Price, S. F., Quiquet, A., Radić, V.,
918 Reese, R., Rounce, D. R., Rückamp, M., Sakai, A., Shafer, C., Schlegel, N.-J., Shannon, S., Smith, R. S.,
919 Straneo, F., Sun, S., Tarasov, L., Trusel, L. D., Van Breedam, J., van de Wal, R., van den Broeke, M.,
920 Winkelmann, R., Zekollari, H., Zhao, C., Zhang, T., and Zwinger, T.: Projected land ice contributions to twenty-
921 first-century sea level rise, *Nature*, 593, 74–82, doi:10.1038/s41586-021-03302-y, 2021.

922 Esri. “Imagery” [basemap]. Scale Not Given. “World Imagery”. October 10, 2024.
923 <https://www.arcgis.com/home/item.html?id=10df2279f9684e4a9f6a7f08f6bac2a9>. (October 22, 2024)

924 Ferguson, R. I.: Sinuosity of supraglacial streams, *Geol. Soc. Am. Bull.*, 84, 251–256, doi:10.1130/0016-
925 7606(1973)84<251:SOSS>2.0.CO;2, 1973.

926 Fischer, M., Huss, M., and Hoelzle, M.: Surface elevation and mass changes of all Swiss glaciers 1980–2010,
927 *Cryosphere*, 9, 525–540, doi:10.5194/tc-9-525-2015, 2015.

928 Fleischer, F., Otto, J.-C., Junker, R. R., and Hölbling, D.: Evolution of debris cover on glaciers of the Eastern
929 Alps, Austria, between 1996 and 2015, *Earth Surf. Process. Landf.*, 46, 1673–1691, doi:10.1002/esp.5065, 2021.

930 Glasser, N. F., Holt, T. O., Evans, Z. D., Davies, B. J., Pelto, M., and Harrison, S.: Recent spatial and temporal
931 variations in debris cover on Patagonian glaciers, *Geomorphology*, 273, 202–216,
932 doi:10.1016/j.geomorph.2016.07.036, 2016.

933 Gleason, C. J., Smith, L. C., Chu, V. W., Legleiter, C. J., Pitcher, L. H., Overstreet, B. T., Rennermalm, A. K.,
934 Forster, R. R., and Yang, K.: Characterizing supraglacial meltwater channel hydraulics on the Greenland Ice
935 Sheet from in situ observations, *Earth Surf. Process. Landf.*, 41, 2111–2122, doi:10.1002/esp.3977, 2016.

936 Gleason, C. J., Yang, K., Feng, D., Smith, L. C., Liu, K., Pitcher, L. H., Chu, V. W., Cooper, M. G., Overstreet,
937 B. T., Rennermalm, A. K., and Ryan, J. C.: Hourly surface meltwater routing for a Greenlandic supraglacial
938 catchment across hillslopes and through a dense topological channel network, *Cryosphere*, 15, 2315–2331,
939 doi:10.5194/tc-15-2315-2021, 2021.

940 Hambrey, M. J.: Supraglacial drainage and its relationship to structure, with particular reference to Charles
941 Rabots Bre, Okstindan, Norway, *Nor. Geogr. Tidsskr.*, 31, 69–77, doi:10.1080/00291957708545319, 1977.

942 Horton, R. E.: Erosional development of streams and their drainage basins; hydrophysical approach to
943 quantitative morphology, *Geol. Soc. Am. Bull.*, 56, 275–370, doi:10.1130/0016-
944 7606(1945)56[275:EDOSAT]2.0.CO;2, 1945.

945 Hugonnet, R., McNabb, R., Berthier, E., Menounos, B., Nuth, C., Girod, L., Farinotti, D., Huss, M., Dussaillant,
946 I., Brun, F., and Kääb, A.: Accelerated global glacier mass loss in the early twenty-first century, *Nature*, 592,
947 726–731, doi:10.1038/s41586-021-03436-z, 2021.

948 Huss, M., Bauder, A., Werder, M., Funk, M., and Hock, R.: Glacier-dammed lake outburst events of Gornesse, Switzerland, *J. Glaciol.*, 53, 189–200, doi.org:10.3189/172756507782202784, 2007.

950 Immerzeel, W. W., Lutz, A. F., Andrade, M., Bahl, A., Biemans, H., Bolch, T., Hyde, S., Brumby, S., Davies, B. J., Elmore, A. C., Emmer, A., Feng, M., Fernández, A., Haritashya, U., Kargel, J. S., Koppes, M., Kraaijenbrink, P. D. A., Kulkarni, A. V., Mayewski, P. A., Nepal, S., Pacheco, P., Painter, T. H., Pellicciotti, F., Rajaram, H., Rupper, S., Sinisalo, A., Shrestha, A. B., Viviroli, D., Wada, Y., Xiao, C., Yao, T., and Baillie, J. E. M.: Importance and vulnerability of the world's water towers, *Nature*, 577, 364–369, doi:10.1038/s41586-019-1822-y, 2020.

956 Irvine-Fynn, T. D. L., Hodson, A. J., Moorman, B. J., Vatne, G., and Hubbard, A. L.: Polythermal glacier hydrology: a review, *Rev. Geophys.*, 49, doi:10.1029/2010RG000350, 2011.

958 [Jiskoot, H., Fox, T. A., and Wychen, W. V.: Flow and structure in a dendritic glacier with bedrock steps, *J. Glaciol.*, 63, 912–928, doi:10.1017/jog.2017.58, 2017.](#)

960 Jobard, S. and Dzikowski, M.: Evolution of glacial flow and drainage during the ablation season, *J. Hydrol.*, 330, 663–671, doi:10.1016/j.jhydrol.2006.04.031, 2006.

962 Karlstrom, L. and Yang, K.: Fluvial supraglacial landscape evolution on the Greenland Ice Sheet, *Geophys. Res. Lett.*, 43, 2683–2692, doi:10.1002/2016GL067697, 2016.

964 Khan, A. L., Xian, P., and Schwarz, J. P.: Black carbon concentrations and modeled smoke deposition fluxes to the bare-ice dark zone of the Greenland Ice Sheet, *Cryosphere*, 17, 2909–2918, doi:10.5194/tc-17-2909-2023, 2023.

967 King, L., Hassan, M. A., Yang, K., and Flowers, G.: Flow routing for delineating supraglacial meltwater channel networks, *Remote Sens.*, 8, 988, doi:10.3390/rs8120988, 2016.

969 Kingslake, J., Ely, J. C., Das, I., and Bell, R. E.: Widespread movement of meltwater onto and across Antarctic ice shelves, *Nature*, 544, 349–352, doi:10.1038/nature22049, 2017.

971 Knighton, A. D.: Channel form adjustment in supraglacial streams, Austre Okstindbreen, Norway, *Arct. Antarct. Alp. Res.*, 17, 451, doi:10.2307/1550870, 1985.

973 Knighton, A. D.: Channel form and flow characteristics of supraglacial streams, Austre Okstindbreen, Norway, *Arct. Alp. Res.*, 13, 295, doi:10.2307/1551036, 1981.

975 Knighton, A. D.: Meandering habit of supraglacial streams, *Geol. Soc. Am. Bull.*, 83, 201–204, doi:10.1130/0016-7606(1972)83[201:MHOSS]2.0.CO;2, 1972.

977 Leeson, A. A., Shepherd, A., Briggs, K., Howat, I., Fettweis, X., Morlighem, M., and Rignot, E.: Supraglacial lakes on the Greenland Ice Sheet advance inland under warming climate, *Nat. Clim. Change*, 5, 51–55, doi:10.1038/nclimate2463, 2015.

980 Leidman, S. Z., Rennermalm, Å. K., Muthyala, R., Guo, Q., and Overeem, I.: The presence and widespread distribution of dark sediment in Greenland Ice Sheet supraglacial streams implies substantial impact of microbial communities on sediment deposition and albedo, *Geophys. Res. Lett.*, 48, 2020GL088444, doi:10.1029/2020GL088444, 2021.

984 Leigh, J. R., Stokes, C. R., Carr, R. J., Evans, I. S., Andreassen, L. M., and Evans, D. J. A.: Identifying and mapping very small (<0.5 km²) mountain glaciers on coarse to high-resolution imagery, *J. Glaciol.*, 65, 873–888, <https://doi.org/10.1017/jog.2019.50>, 2019.

987 Leinss, S. and Bernhard, P.: TanDEM-X: Deriving InSAR height changes and velocity dynamics of Great Aletsch Glacier, *IEEE J. Sel. Top. Appl. Earth Obs. Remote Sens.*, 14, 4798–4815, <https://doi.org/10.1109/JSTARS.2021.3078084>, 2021.

990 Linsbauer, A., Huss, M., Hodel, E., Bauder, A., Fischer, M., Weidmann, Y., Bärtschi, H., and Schmassmann, E.:
 991 The new Swiss glacier inventory SGI2016: from a topographical to a glaciological dataset, *Front. Earth Sci.*, 9,
 992 doi:10.3389/feart.2021.704189, 2021.

993 Mantelli, E., Camporeale, C., and Ridolfi, L.: Supraglacial channel inception: modeling and processes, *Water*
 994 *Resour. Res.*, 51, 7044–7063, doi:10.1002/2015WR017075, 2015.

995 Marston, R. A.: Supraglacial stream dynamics on the Juneau Icefield, *Ann. Am. Assoc. Geogr.*, 73, 597–608,
 996 doi:10.1111/j.1467-8306.1983.tb01861.x, 1983.

997 MeteoSwiss: <https://www.meteoswiss.admin.ch/>, last access: 1 February 2024.

998 Micheletti, N. and Lane, S. N.: Water yield and sediment export in small, partially glaciated Alpine watersheds
 999 in a warming climate, *Water Resour. Res.*, 52, 4924–4943, doi: 10.1002/2016WR018774, 2016.

1000 Nienow, P., Sharp, M., and Willis, I.: Seasonal changes in the morphology of the subglacial drainage system,
 1001 Haut Glacier d’Arolla, Switzerland, *Earth Surf. Process. Landf.*, 23, 825–843,
 1002 [https://doi.org/10.1002/\(SICI\)1096-9837\(199809\)23:9<825::AID-ESP893>3.0.CO;2-2](https://doi.org/10.1002/(SICI)1096-9837(199809)23:9<825::AID-ESP893>3.0.CO;2-2), 1998.

1003 [Paul, F., Rastner, P., Azzoni, R. S., Diolaiuti, G., Fugazza, D., Le Bris, R., Nemec, J., Rabatel, A., Ramusovic,](#)
 1004 [M., Schwaizer, G., and Smiraglia, C.: Glacier inventory of the Alps from Sentinel-2, shape files \[dataset\],](#)
 1005 [PANGAEA, doi:10.1594/PANGAEA.909133, 2019](#)

1006 Pitcher, L. H. and Smith, L. C.: Supraglacial Streams and Rivers, *Annu. Rev. Earth Planet. Sci.*, 47, 421–452,
 1007 doi:10.1146/annurev-earth-053018-060212, 2019.

1008 Rippin, D. M., Pomfret, A., and King, N.: High resolution mapping of supra-glacial drainage pathways reveals
 1009 link between micro-channel drainage density, surface roughness and surface reflectance, *Earth Surf. Process.*
 1010 *Landf.*, 40, 1279–1290, doi:10.1002/esp.3719, 2015.

1011 Rounce, D. R., Hock, R., Maussion, F., Hugonnet, R., Kochtitzky, W., Huss, M., Berthier, E., Brinkerhoff, D.,
 1012 Compagno, L., Copland, L., Farinotti, D., Menounos, B., and McNabb, R. W.: Global glacier change in the 21st
 1013 century: Every increase in temperature matters, *Science*, 379, 78–83, doi:10.1126/science.abo1324, 2023.

1014 Ryan, J. C., Hubbard, A., Stibal, M., Irvine-Fynn, T. D., Cook, J., Smith, L. C., Cameron, K., and Box, J.: Dark
 1015 zone of the Greenland Ice Sheet controlled by distributed biologically-active impurities, *Nat. Commun.*, 9, 1065,
 1016 doi:10.1038/s41467-018-03353-2, 2018.

1017 Seaberg, S. Z., Seaberg, J. Z., Hooke, R. L., and Wiberg, D. W.: Character of the englacial and subglacial
 1018 drainage system in the lower part of the ablation area of Storglaciären, Sweden, as Revealed by Dye-Trace
 1019 Studies, *J. Glaciol.*, 34, 217–227, doi:10.3189/S0022143000032263, 1988.

1020 Smith, L. C., Chu, V. W., Yang, K., Gleason, C. J., Pitcher, L. H., Rennermalm, A. K., Legleiter, C. J., Behar, A.
 1021 E., Overstreet, B. T., Moustafa, S. E., Tedesco, M., Forster, R. R., LeWinter, A. L., Finnegan, D. C., Sheng, Y.,
 1022 and Balog, J.: Efficient meltwater drainage through supraglacial streams and rivers on the southwest Greenland
 1023 Ice Sheet, *Proc. Natl. Acad. Sci.*, 112, 1001–1006, doi:10.1073/pnas.1413024112, 2015.

1024 Sommer, C., Malz, P., Seehaus, T. C., Lippl, S., Zemp, M., and Braun, M. H.: Rapid glacier retreat and
 1025 downwasting throughout the European Alps in the early 21st century, *Nat. Commun.*, 11, 3209,
 1026 doi:10.1038/s41467-020-16818-0, 2020.

1027 St Germain, S. L. and Moorman, B. J.: Long-term observations of supraglacial streams on an Arctic glacier, *J.*
 1028 *Glaciol.*, 65, 900–911, doi:10.1017/jog.2019.60, 2019.

1029 Swift, D. A., Nienow, P. W., Spedding, N., and Hoey, T. B.: Geomorphic implications of subglacial drainage
 1030 configuration: rates of basal sediment evacuation controlled by seasonal drainage system evolution, *Sediment.*
 1031 *Geol.*, 149, 5–19, doi:10.1016/S0037-0738(01)00241-X, 2002.

1032 Tepes, P., Gourmelen, N., Nienow, P., Tsamados, M., Shepherd, A., and Weissgerber, F.: Changes in elevation
1033 and mass of Arctic glaciers and ice caps, 2010–2017, *Remote Sens. Environ.*, 261, 112481,
1034 doi:10.1016/j.rse.2021.112481, 2021.

1035 The GlaMBIE Team: Community estimate of global glacier mass changes from 2000 to 2023, *Nature*, 1–7,
1036 doi:10.1038/s41586-024-08545-z, 2025.

1037 Willis, I.C.: Intra-annual variations in glacier motion: a review, *Prog. Phys. Geogr.*, 19,
1038 doi:10.1177/030913339501900104, 1995.

1039 Wouters, B., Gardner, A. S., and Moholdt, G.: Global glacier mass loss during the GRACE satellite mission
1040 (2002–2016), *Front. Earth Sci.*, 7, 2019.

1041 Yang, K. and Smith, L. C.: Internally drained catchments dominate supraglacial hydrology of the southwest
1042 Greenland Ice Sheet, *J. Geophys. Res.-Earth Surf.*, 121, doi:10.1002/2016JF003927, 2016.

1043 Yang, K. and Smith, L. C.: Supraglacial streams on the Greenland Ice Sheet delineated from combined spectral-
1044 shape information in high-resolution satellite imagery, *IEEE Geosci. Remote Sens. Lett.*, 10, 801–805,
1045 doi:10.1109/LGRS.2012.2224316, 2013.

1046 Yang, K., Smith, L. C., Andrews, L. C., Fettweis, X., and Li, M.: Supraglacial drainage efficiency of the
1047 Greenland Ice Sheet estimated from remote sensing and climate models, *J. Geophys. Res.-Earth Surf.*, 127,
1048 e2021JF006269, doi:10.1029/2021JF006269, 2022.

1049 Yang, K., Smith, L. C., Chu, V. W., Gleason, C. J., and Li, M.: A caution on the use of surface digital elevation
1050 models to simulate supraglacial hydrology of the Greenland Ice Sheet, *IEEE J. Sel. Top. Appl. Earth Observ.*
1051 *Remote Sens.*, 8, 5212–5224, doi:10.1109/JSTARS.2015.2483483, 2015.

1052 Yang, K., Smith, L. C., Chu, V. W., Pitcher, L. H., Gleason, C. J., Rennermalm, A. K., and Li, M.: Fluvial
1053 morphometry of supraglacial river networks on the southwest Greenland Ice Sheet, *GISci. Remote Sens.*, 53,
1054 459–482, doi:10.1080/15481603.2016.1162345, 2016.

1055 Yang, K., Smith, L. C., Cooper, M. G., Pitcher, L. H., As, D. van, Lu, Y., Lu, X., and Li, M.: Seasonal evolution
1056 of supraglacial lakes and rivers on the southwest Greenland Ice Sheet, *J. Glaciol.*, 67, 592–602,
1057 doi:10.1017/jog.2021.10, 2021.

1058 Yang, K., Smith, L. C., Karlstrom, L., Cooper, M. G., Tedesco, M., van As, D., Cheng, X., Chen, Z., and Li, M.:
1059 A new surface meltwater routing model for use on the Greenland Ice Sheet surface, *Cryosphere*, 12, 3791–3811,
1060 doi:10.5194/tc-12-3791-2018, 2018.

1061 Yang, K., Smith, L. C., Sole, A., Livingstone, S. J., Cheng, X., Chen, Z., and Li, M.: Supraglacial rivers on the
1062 northwest Greenland Ice Sheet, Devon Ice Cap, and Barnes Ice Cap mapped using Sentinel-2 imagery, *Int. J.*
1063 *Appl. Earth Obs. Geoinf.*, 78, 1–13, doi:10.1016/j.jag.2019.01.008, 2019.

1064 Yang, K., Sommers, A., Andrews, L. C., Smith, L. C., Lu, X., Fettweis, X., and Li, M.: Intercomparison of
1065 surface meltwater routing models for the Greenland Ice Sheet and influence on subglacial effective pressures,
1066 *Cryosphere*, 14, 3349–3365, doi:10.5194/tc-14-3349-2020, 2020.

1067 Zekollari, H., Huss, M., and Farinotti, D.: Modelling the future evolution of glaciers in the European Alps under
1068 the EURO-CORDEX RCM ensemble, *Cryosphere*, 13, 1125–1146, doi:10.5194/tc-13-1125-2019, 2019.

1069 Zemp, M., Huss, M., Thibert, E., Eckert, N., McNabb, R., Huber, J., Barandun, M., Machguth, H., Nussbaumer,
1070 S. U., Gärtner-Roer, I., Thomson, L., Paul, F., Maussion, F., Kutuzov, S., and Cogley, J. G.: Global glacier mass
1071 changes and their contributions to sea-level rise from 1961 to 2016, *Nature*, 568, 382–386, doi:10.1038/s41586-
1072 019-1071-0, 2019.